AECL-7241

ATOMIC ENERGY OF CANADA LIMITED

L'ÉNERGIE ATOMIQUE DU CANADA LIMITÉE

REACTOR PHYSICS MEASUREMENTS WITH 19-ELEMENT ThO_2-$^{235}UO_2$ CLUSTER FUEL IN HEAVY WATER MODERATOR

Mesures en physique des réacteurs effectuées avec une barre de combustible comprenant 19 éléments de ThO_2-$^{235}UO_2$ employant de l'eau lourde comme modérateur

P.M. FRENCH

Chalk River Nuclear Laboratories

Laboratoires nucléaires de Chalk River

Chalk River, Ontario

February 1985 février

ATOMIC ENERGY OF CANADA LIMITED

REACTOR PHYSICS MEASUREMENTS WITH 19-ELEMENT ThO_2-$^{235}UO_2$ CLUSTER FUEL IN HEAVY WATER MODERATOR

P.M. French*

*presently with Atomic Energy Control Board

Chalk River Nuclear Laboratories
CHALK RIVER, Ontario, K0J 1J0
1985 February

AECL-7241

L'ENERGIE ATOMIQUE DU CANADA, LIMITEE

Mesures en physique des réacteurs effectuées avec une barre de combustible comprenant 19 éléments de ThO_2-$^{235}UO_2$ employant de l'eau lourde comme modérateur

par

P.M. French*

Résumé

Des mesures concernant la physique des réseaux à faible puissance ont été réalisées avec une barre de combustible munie de 19 éléments renfermant de l'oxyde de thorium enrichi de 1,45% en poids d'oxyde d'uranium 235 (enrichissement de 93%), cette barre étant placée dans un coeur de réacteur simulé employant de l'eau lourde comme modérateur et comme caloporteur. Les expériences ont été conçues dans le but d'obtenir des données applicables à l'irradiation dans les réacteurs de puissance et d'avoir quelques informations de base en ce qui concerne la physique des combustibles à base de thorium et d'uranium.

La mesure détaillée des cellules de réseau comprenait la détermination de la répartition relative des activations du cuivre ainsi que des rapports d'activité de l'indium 116 et du manganèse 56 d'une part et du lutétium 177 et du manganèse 56 d'autre part, relativement à un lieu de référence thermique. On a déduit des résultats obtenus les paramètres de spectre neutronique de Westcott. Ce rapport décrit également les effets de la réactivité dans le coeur, les facteurs des pics de flux à l'extrémité des grappes et les effets macroscopiques de la perturbation du coeur associés au combustible à base de thorine ayant un grand pouvoir absorbant.

On trouvera, enfin, dans ce rapport, le résumé de quelques calculs théoriques concernant le flux et montrant un bon accord avec les résultats expérimentaux.

Laboratoires nucléaires de Chalk River
Chalk River, Ontario, KOJ 1JO

Février 1985

AECL-7241

*Actuellement en poste à la Commission de contrôle de l'énergie atomique

ATOMIC ENERGY OF CANADA LIMITED

REACTOR PHYSICS MEASUREMENTS WITH 19-ELEMENT ThO_2-$^{235}UO_2$ CLUSTER FUEL IN HEAVY WATER MODERATOR

by

P.M. French

ABSTRACT

Low power lattice physics measurements have been performed with a single rod of 19-element thorium oxide fuel enriched with 1.45 wt.% $^{235}UO_2$ (93% enriched) in a simulated heavy water moderated and cooled power reactor core. The experiments were designed to provide data relevant to a power reactor irradiation and to obtain some basic information on the physics of uranium-thorium fuel material.

Detailed lattice cell measurements included relative copper activation distributions and both $^{116}In/^{56}Mn$ and $^{177}Lu/^{56}Mn$ activity ratios relative to a thermal reference location. Westcott neutron spectrum parameters were inferred from the results. Core reactivity effects, bundle end flux peaking factors and macroscopic core perturbation effects associated with the heavily absorbing thoria fuel are also reported.

Some theoretical flux calculations are summarized and show reasonable agreement with experiment.

Chalk River Nuclear Laboratories
CHALK RIVER, Ontario, K0J 1J0
1985 February

AECL-7241

*presently with the Atomic Energy Control Board

REACTOR PHYSICS MEASUREMENTS WITH 19-ELEMENT ThO_2-$^{235}UO_2$ CLUSTER FUEL IN HEAVY WATER MODERATOR

by

P.M. French

TABLE OF CONTENTS

LIST OF TABLES

LIST OF FIGURES

LIST OF FIGURES (continued)

REACTOR PHYSICS MEASUREMENTS WITH 19-ELEMENT ThO_2-$^{235}UO_2$ CLUSTER FUEL IN HEAVY WATER MODERATOR

by

P.M. French*

1. INTRODUCTION

Future possible increases in uranium price, the question of continuing supplies at adequate levels, and concerns over satisfactory uranium reserves have provided an incentive to examine advanced fuel cycles that will conserve this resource (1,2).

Thorium utilization in thermal reactors such as CANDU** is particularly attractive. These reactors are inherently neutron economic and can be optimized to operate as near-breeders, recycling ^{233}U bred from ^{232}Th. Initially the thorium must be enriched with either fissile uranium or plutonium but as the equilibrium fuel cycle is approached more ^{233}U is recycled, thus reducing the demand for external fissile topping. Recent studies of thorium cycles in CANDU-PHW** reactors have been carried out (3,4) and development and demonstration programs are being planned.

A pilot irradiation program in the Douglas Point reactor had been planned using up to 10 bundles of 19-element thorium oxide fuel enriched with 1.45 wt.% $^{235}UO_2$ (93% enriched) to provide information on fuel behaviour and experience with thorium fuel management and handling (5). Prior to this irradiation, lattice experiments were performed in the ZED-2 low power critical facility to provide physics data relevant to the power reactor tests and to obtain some basic information on the physics of uranium-thorium fuel material.

This report summarizes the results of these low power experiments made with a single thorium rod assembly in a mock-up Douglas Point core. Reactivity effects associated with the substitution of thorium assemblies for a natural uranium rod were measured as changes in critical moderator level. Detailed measurements using activation foils and wires were made throughout a lattice cell and included relative copper activity distributions, bundle and flux peaking factors, and $^{116}In/^{56}Mn$ and $^{177}Lu/^{56}Mn$ activity ratios relative to a thermal reference location. Westcott spectral indices (6) T_n and r were inferred from these latter experimental results. Finally, detailed core perturbation effects were obtained from macroscopic copper activity results.

---

* Presently with the Atomic Energy Control Board

**CANada Deuterium Uranium-Pressurized Heavy Water

The results reported here are complemented by reference 7 which describes measurements of the conversion ratio for this same fuel.

2. FUEL AND LATTICE CONFIGURATION

2.1 Lattice Description

All measurements were made in the ZED-2 reactor at the center of a 77-rod, D_2O cooled, rod-centered reference lattice shown in Fig. 1; the lattice pitch was 22.86 cm (9 in.) square. The central test rod, which contained the measurement bundles, was surrounded by a buffer region of eight rods housing D_2O cooled 19-element, natural UO_2 Douglas Point production fuel bundles loaned by Ontario Hydro. The remainder of the lattice consisted of 44 D_2O cooled 28-element, natural UO_2 fuel assemblies (8,9) surrounded by 24 natural U metal, full length ZEEP rods both shown in Fig. 2. Each of the 28-element rods was composed of five bundles (49.67 cm in length) stacked inside a housing assembly consisting of an Al pressure tube surrounded by an Al calandria tube. The base of the fuel was at 15 cm elevation from the floor of the reactor vessel in each rod.

Figure 3 shows a cross-sectional view of a 19-element natural UO_2 Douglas Point production fuel bundle in an aluminium housing tube assembly. The 18 outer elements in each bundle were arranged in two circular rings of six and twelve elements with pitch circle diameters of 3.302 cm and 6.360 cm respectively. The bundle was formed by welding these elements to two Zircaloy-4 end plate spiders, 0.160 cm thick, and measured 49.55 cm in length. Each fuel element consisted of a stack of dished ended pellets (10.60 g/cm^3 density, 1.425 cm dia.) contained in a Zircaloy-4 sheath (1.523 cm O.D., 0.038 cm wall) with welded Zircaloy-4 end caps. The element length was 49.23 cm, and the fuel length 48.1 cm (nominal); axial fuel stack clearance was 0.23 cm (nominal). Bundle end region detail is shown in Fig. 4.

The 19-element bundles were suspended in double walled Al calandria/pressure tube assemblies (dimensions in Fig. 3) with the base of the fuel at 15 cm elevation from the floor of the reactor vessel.

The moderator temperature and purity varied between 19.45°C and 20.83°C and 99.636 and 99.624 weight % D_2O respectively during the experimental program.

2.2 Measurement Assemblies

Measurements were made with three different fuel configurations in the central rod: five 19-element Douglas Point natural UO_2 bundles ("reference" configuration); two 19-element thorium bundles sandwiched between natural UO_2 clusters to simulate the proposed thoria irradiation at Douglas Point; and five thorium bundles. The thorium bundles were geometrically identical to the 19-element natural UO_2 clusters. The fuel, however, was a mixture of ThO_2 and 1.45 wt.% UO_2, 93.2% enriched in U-235 and the measured density was 9.67 $\pm$ 0.02 g/cm^3.

Specially fabricated "demountable" bundles (one thorium and two UO_2) were used for foil activation measurements in the fuel. Each of the UO_2 measurement bundles was composed of 15 elements (47.73 cm fuel length) with welded end caps having threaded projections, and four with removable "O" ring fitted Al end caps to allow access to the fuel stacks; the bundle (overall length 49.38 cm) was formed by bolting the welded elements to two Zircaloy-2 end plates. The sheaths were of Zircaloy-2 1.522 cm O.D., 0.046 cm wall (welded elements), and 0.025 cm wall thickness (accessible elements). The fuel diameter was 1.421 cm, density 10.45 g/cm^3.

The thorium measurement bundle was similar in construction to the demountable UO_2 bundles. Fourteen elements had welded end caps with threaded projections and measured 49.28 cm long. The fuel length was 48.1 cm nominal with 0.23 cm axial fuel stack gap. The five accessible elements had removable Al "O" ring fitted end caps and were the same length; fuel length was 47.5 cm and the sheath diameters were identical to those for the production bundles. Demountable bundle end region details are shown in Fig. 5 for the configuration with a thorium bundle adjacent to a natural UO_2 bundle. For this configuration note that the production and demountable bundle end plate junctions in the central rod were at core elevations 63.85 cm and 163.94 cm respectively (Fig. 9). Corresponding fuel end elevations were at 63.01 and 64.46 cm for the production bundles, and 162.40 and 165.30 cm for the demountable bundle junction. The demountable bundles were housed in Al calandria/pressure tube assemblies identical to those described above for the 19-element production fuel.

The UO_2 and thoria demountable bundles are illustrated in Figs. 6 and 7 respectively and show the various components of each partially disassembled bundle.

3. CRITICAL HEIGHT MEASUREMENTS

3.1 Measurements

Critical moderator level measurements were performed for the following lattice configurations.

(1) Reference lattice, D_2O cooled (Fig. 1).

(2) Reference lattice with central 19-element UO_2 rod air cooled.

(3) Reference lattice but with central rod replaced by a fuel assembly containing five, 19-element thorium bundles (air or D_2O cooled).

(4) As for (3), but central rod containing three natural UO_2 assemblies in positions No. 1, 4 and 5 (Fig. 9) and two thorium bundles in positions No. 2 and 3 - central rod air or D_2O cooled.

(5) As for (4), but central rod containing only one thorium bundle at position No. 3, remainder of rod containing natural UO_2 - D_2O cooled.

(6) A critical height measurement was also made in a D_2O cooled lattice with the nine central 19-element assemblies replaced with 28-element rods: i.e. 53, 28-element assemblies driven with 24 ZEEP rods.

3.2 Results

The measured data are listed in Table 1 together with respective heavy water moderator temperature and purity conditions during each experiment.

The results indicate that the thorium fuel is a net absorber, and that the coolant void effect is substantially lower than that of natural UO_2.

4. DETAILED CU ACTIVITY MEASUREMENTS

Detailed lattice cell neutron flux distributions were measured with Cu activation foils and wires in each of the three central cell configurations, namely: five bundles of natural UO_2, five thoria bundles, and two thoria bundles sandwiched between three UO_2 (Fig. 9).

Core macroscopic measurements were made only in the first and third configurations to assess the perturbation effects in a simulation of the proposed power reactor irradiations.

4.1 Location of Detectors

Detailed activity distributions in a lattice cell and macroscopic measurements across the core were determined using 1.13 cm diameter, 0.025 cm thick Cu foils at interstitial moderator locations; 1.43 cm diameter, 0.013 cm thick Cu in the fuel; and 1 cm long, 0.076 cm diameter Cu wires on an Al framework in the central cell. Foils located between fuel pellets were shielded with thin (0.003 cm) Al foils to prevent fission product contamination. Typical macroscopic core locations are shown in Fig. 1, while the detector arrangement in the central cell is outlined in Figs. 8 and 9. Note that measurements in fuel were made both in a thorium bundle and in two neighbouring natural UO_2 bundles for the central rod configuration simulating the proposed power reactor thoria irradiation.

Detectors used for radial measurements were located at an elevation near the axial central plane of one of the demountable bundles ($\sim$ 140 cm elevation) close to the core axial flux peak. Slight differences in elevation between groupings of detectors were corrected either by interpolation between pairs of activations at different elevations or by using cosine parameters obtained from least squares fitting to a measured axial distribution.

4.2 Determination of Activities

Following neutron activation, the 12.75 h ^{64}Cu γ -ray foil activities were determined using a pair of 5.08 cm diameter (2.54 cm thick) NaI (Tl) scintillation detector systems in $\sim 4\pi$ geometry. An automatically restacking sample changer inserted acrylic sample trays, each containing an active foil, in sequence in a small gap (<2 cm) between the faces of the two scintillators. The output from each detector was computer analyzed to correct each foil for decay, counter dead-time losses, foil mass, and background. A waiting period of several hours following an irradiation, before counting, ensured that the activity from ^{66}Cu had decayed to a negligible amount.

4.3 Results

Relative copper activations in the central cells, normalized to 1.0 at the central fuel pin location in the central rod, are summarized in Tables 2 to 4 for the three experimental configurations at the central site: five UO_2, two thoria sandwiched between three UO_2, and five thoria bundles. All copper activities have been corrected to the elevation of the copper in the fuel ($\sim$140 cm). The cell activity distributions are also plotted in Figs. 10 and 11 for two of the fuel configurations; the two and five bundle flux shapes are very similar and only the former has been plotted. Note that relative errors are about $\pm$ 1%.

Macroscopic copper activations across the reactor core for the five UO_2 and two thoria central configurations are summarized in Tables 5 and 6. The flux perturbation in the reference core caused by the substitution of a rod containing two thorium bundles at the center of the core is better represented using a flux ratio technique. Therefore, flux perturbation factors [F(r,z)] have been defined as follows:

$$F(r,z) = \left[\frac{A(r,z)}{A(R',z)}\right]_{\text{Thorium lattice}} \Big/ \left[\frac{A(r,z)}{A(R',z)}\right]_{UO_2 \text{ lattice}}$$

where A is the measured activity, r and z refer to radial and axial co-ordinates and R' is an unperturbed radial location. Normalizing each experiment, by elevation, to an unperturbed location corrects the perturbation factors for critical height and thus macroscopic axial flux differences between the perturbed and unperturbed lattices.

The flux perturbation factor results are summarized in Tables 7 and 8, and in Figs. 12 and 13. Relative errors are about $\pm$ 1.3%. The results clearly show the substantial flux depression in the central fuel rod, about 35 to 50%, when thoria replaces UO_2. The perturbation extends to the nearest neighbour UO_2 lattice sites where the thermal flux in the fuel is depressed about 5%.

Flux perturbation factors and radial flux depression across both a thorium and natural UO_2 bundle have been calculated (10) using the cell code LATREP (11) and PERIGEE (12), a three-dimensional, two-group diffusion code. The agreement with experiment is generally quite good. Calculated relative fission rates in the fuel pins are compared with copper foil activities in Figs. 10 and 11 and the agreement is within 2%. Calculated flux perturbation factors are compared with experiment in Fig. 12; agreement is within 2% in the thorium fuel and within 1% at moderator locations.

5. BUNDLE END FLUX PEAKING MEASUREMENTS

5.1 Measurements

Flux peaking measurements were performed for only one of the central rod fuel configurations: two thorium bundles sandwiched between 19-element natural UO_2 clusters to simulate the thorium irradiation in a power reactor. Cu foils (1.422 cm diameter, 0.013 cm thick) were placed between fuel pellets axially along certain elements in adjacent thorium and

natural UO_2 demountable bundles; typical axial foil locations in representative elements are detailed in Fig. 5. Since a limited number of demountable measurement elements were available, copper foil peaking measurements at the fuel ends have been made only in the outer elements of both bundle types (elements 1 and 5, Fig. 8) and in the intermediate element of the thorium bundle (element 4). During irradiation, the copper was shielded from fission product contamination with thin (0.003 cm) Al foils, which were removed prior to counting the neutron activation decay gammas.

Measurements using foils between fuel pellets in the demountable bundle overestimate production fuel flux peaking since the end caps and end plates are thicker and increase the gap between the fuel in adjacent bundles. To circumvent this difficulty, a copper wire was positioned axially at the junction between production fuel bundles in the coolant space between the intermediate and outer fuel rings.

A similar wire was irradiated at the junction of two demountable bundles and compared with foil activation measurements. A correction factor was thus obtained to convert all the wire activation results in the coolant space to equivalent flux peaking in the fuel.

The copper wires (0.216 cm diameter) were positioned in straightened aluminum tubes (0.476 cm O.D., 0.295 cm I.D.) located midway between four adjacent fuel elements using annular teflon collars (0.808 cm O.D.) equally spaced along the tubes (Figs. 3 and 14). Each wire was 85 cm long and in one case extended the full length of a production UO_2 bundle (position Number 1, Fig. 9), projecting about 35 cm into the upper thorium production bundle; the other wire was similarly located between a thorium demountable (position Number 3) and upper UO_2 demountable bundle.

5.2 Determination of Activities

The Cu foil activities were determined in the normal manner (see Section 4.2).

The ^{64}Cu activity distribution along the wires was measured using a wire scanner (13). Each wire was clamped at both ends in the scanner carriage and automatically moved in discrete steps across a collimated 5.1 cm diameter, 2.54 cm thick NaI scintillation detector mounted in a lead shield. The wire position over the collimator and distance from the detector face were fixed using guide bars. The activities of the wires were measured at intervals of 0.498 cm over a 100 s counting period and recorded on paper tape. These outputs were computer analyzed to correct each count for counter background and isotopic decay. Statistical errors in counting were typically < 1%.

5.3 Results and Discussion

Cu foil activity results, measured between fuel pellets near the ThO_2-$^{235}UO_2$ and natural UO_2 demountable bundle junctions at the central rod site, are shown in Table 9. The results have been corrected for macroscopic axial flux shape using a Cu foil activity distribution near the edge of the core, away from the large central cell axial perturbation. The element flux peaking factor at a distance z from the end of the fuel is defined as $A(z)/A(z_o)$ where z_o is a location unperturbed by the end flux peaking, normally the element axial mid-plane. Since the activities in Table 9 have been normalized to 1.0 near the mid-plane in each element, the results read element flux peaking factors directly.

The corresponding Cu wire axial activity distribution measured in the coolant space was corrected for axial core flux shape, normalized to 1.00 at the thorium demountable bundle mid-plane, and compared with the Cu foil peaking factors in the fuel elements. Since the peaking is localized near the bundle end region, a simple linear correction factor applied to the wire activation results within 5 cm of the fuel ends gave good agreement with the Cu foils in the fuels. The empirical adjustment corrected the wire results to Cu activities at the bundle mid-planes, and applied a linear correction factor which varied from 1.0, 5 cm from the fuel stack end, to a value equal to the ratio of foil to wire peaking factors at the fuel ends. The demountable bundle normalized wire results, together with the Cu foil data, are shown in Figs. 15 and 16.

Since a limited number of demountable elements were available, Cu foil peaking measurements to the fuel ends have been made only in the outer elements of both bundle types, and in the intermediate element of the ThO_2-$^{235}UO_2$ fuel. Consequently, corrected wire activation peaking factor results have been inferred only in the outer fuel ring of natural UO_2 bundles and the outer two rings in the thorium fuel. The outer element results quoted, however, are the important ones from the element power rating point of view. The maximum thermal neutron flux in adjacent fuel bundles occurs at the outer element ends; although flux peaking factors are highest in the central fuel elements, the large radial flux depression across a bundle reduces the absolute magnitude of the flux at these locations.

The appropriate correction factors were applied to the wire activation results for the configuration with a natural UO_2 production bundle abutting a thorium production bundle. The results are summarized in Figs. 17 and 18. Again, the wire results have been corrected for axial core flux shape and normalized to 1.0 at the bundle mid-plane. Fuel end flux peaking factors are 1.46 ± 0.04 and 1.82 ± 0.04 for the outer and intermediate thorium production fuel elements respectively, and 1.11 ± 0.03 for the outer element of the adjacent natural UO_2 production bundle.

Errors in individual Cu foil activities, based on counting reproducibility and errors in relative Cu content, were typically $\pm$ 0.6%.

The uncertainty in the relative macroscopic axial flux shape correction was estimated to be $\sim \pm$ 0.5% based on the flatness of the Cu wire activity distributions in the unperturbed portion of the bundle after correction. Thus the Cu foil peaking factor ratios are estimated to have an uncertainty of $\sim \pm$ 1.0%.

Although the statistical counting errors associated with the Cu wire activities were $\sim \pm$ 0.6%, other effects such as wire non-uniformity and counting geometry resulted in a "scatter" of about $\pm$ 1% in the activation distribution. Coupled with the uncertainty in the axial correction, and the estimated error in wire positioning ($\sim \pm$ 1%), the uncorrected wire peaking factor uncertainty is $\sim \pm$ 1.5%. Thus the wire-to-foil normalization correction error is estimated to be $\sim \pm$1.8% and the uncertainty in the corrected peaking factors about $\pm$ 2.3% for elements in the production bundles.

A correction to the wire activities for collimator resolution was considered unnecessary and has not been made. The correction is important only near the fuel stack ends, where the magnitude of the flux is changing, and in this region the activities have been normalized to the Cu foil results, obviating the need for a resolution correction.

The results of the wire and foil measurements at the mid-plane locations, away from the bundle ends, show clearly the extent of the axial flux depression in the thorium bundle, a net absorber. The thermal neutron flux is reduced about 33% in the outer element of the thorium fuel, compared to that in an adjacent (axial) UO_2 element.

Axial thermal neutron flux distributions have been calculated (14) in each fuel ring into the bundle end regions separating the demountable thorium and natural UO_2 bundles. Calculations were performed with the PEAKAN code (15) which employs collision probability methods to solve the transport equations in R-Z geometry. The CE-HAMMER cell code (16) was used to obtain input four-group cross sections for the various material regions in the PEAKAN representation. Calculated flux peaking factor results are listed in Table 10 together with the available experimental data for comparison. Outer element peaking factors agree quite well with the Cu foil data but underpredict the flux peaking in the intermediate fuel ring of the thorium bundle. Note that the copper activity results have been corrected for epithermal activation, a large effect in the thorium fuel due to substantial spectral hardening (see Section 6), and experimental thermal neutron density ratios have been quoted in the table.

6. SPECTRUM MEASUREMENTS

6.1 Measurements

Neutron spectrum data were obtained from activation measurements with ^{176}Lu and ^{115}In resonance detectors, and ^{55}Mn, essentially a 1/v absorber. Composite packages containing thin Lu-Mn-Al and In-Al alloy foils were irradiated together at various locations in the core and on a rotating wheel at the thermal reference location in the D_2O moderator, outside the reactor core. At the reference site, the neutron spectrum was essentially a Maxwellian distribution with the temperature assumed equal to the physical moderator temperature.

Spectral effects were interpreted by expressing the resonance and 1/v activation results as ratios, and by using the Westcott formalism (6) to obtain the parameters r, the fractional epithermal neutron density, and T_n, the effective neutron temperature of a Maxwellian distribution of neutrons. The relative foil activity ratios are related to the neutron spectral parameters by the following expressions:

$$R_{Mn}^{In} = \frac{(A_{In}/A_{Mn})_x}{(A_{In}/A_{Mn})_{th}} \quad \text{and} \quad R_{Mn}^{Lu} = \frac{(A_{Lu}/A_{Mn})_x}{(A_{Lu}/A_{Mn})_{th}}$$

where x refers to the measurement position in the lattice cell, th to the thermal reference location, and where A, the foil activity, is given in Westcott notation by:

$$A \quad G_t\, g(T_n) + G_r\, s_o\, r\sqrt{T_n/T_o}$$

G_t and G_r are the thermal and resonance foil self-shielding factors respectively. $g(T_n)$ denotes the temperature dependence of the Westcott g value for In and Lu. The method is described in detail by Bigham (17).

At the reference location, $r\sqrt{T_n/T_o}$ was determined from a Cd ratio measurement (18) with thin In-Al foils; g values were taken from Westcott (6). G_t was calculated using Hanna's method (19) and $G_r s_o$

was determined from the Cd ratio measurement method described by Walker (20), using thin deposited Au and In foils as standards. A computer program was used to obtain T_n and $r\sqrt{T_n/T_o}$ values from the measured activity ratios.

Activation measurements were made using composite foil packages containing 0.013 cm thick 1 wt.% In-Al alloy and 0.025 cm thick 10 wt.% Lu - 5 wt.% Mn-Al alloy foils. All foil packages were wrapped in 0.003 cm thick Al foil to prevent fission product contamination from the fuel, and were irradiated between fuel pellets at the central rod site in the 19-element natural UO_2 and/or Thorium demountable bundles, at rod site K2E in a demountable 19-element natural UO_2 bundle, on the calandria tube surfaces at each rod site, at moderator locations, and on a rotating wheel at the thermal reference location. Foil diameters were 1.422 cm in the fuel and 1.295 cm elsewhere.

Representative foil locations in a typical lattice are shown in Fig. 8. In one experiment, where the central site contained five thorium bundles, measurements were also made at various moderator sites near the center of the core; detector packages were secured to a light Al framework extending from the central site at the same axial location as packages in the fuel. In another experiment, measurements were made between fuel pellets near the junction between the thorium and natural UO_2 bundles, in both fuel bundles, to provide spectral information in regions of thermal flux peaking. Small corrections to foils at different axial locations were determined from measurements with Cu foils in an Al thimble located in the moderator near the central rod.

At the thermal reference location $r\sqrt{T_n/T_o}$ was determined from Cd ratio measurements with pairs of 1.13 cm diameter, 0.013 cm thick 1 wt.% In-Al alloy foils, one foil in a Cd box and one in Al (0.076 cm thick walls).

6.2 Determination of Activities

The gamma-ray activities of the irradiated foils were determined using the counter system described earlier (Section 4.2). Since the alloyed foils were not uniform in composition, the relative isotopic content of each detector was determined from relative activities after irradiation on a rotating wheel in the NRU reactor (21) thermal column.

The 12.75 h ^{64}Cu activity, 6.71 d ^{177}Lu activity, and the 54 minute ^{116}In isomeric activity were determined by counting with an effective bias level of ~50 keV. The 2.58 h ^{56}Mn activity was determined at a bias level of ~500 keV to exclude all Lu activities in the Lu-Mn-Al composite foils. The 2.6×10^{10} year ^{176}Lu background activity was determined by counting prior to irradiation, and a correction made.

The In foils were counted beginning ~ one hour after irradiation. The Mn component of the Lu-Mn-Al composite foils was counted three hours after irradiation. The Lu component was counted two or three days after the irradiation to ensure that both the short-lived ^{176}Lu activity and the ^{56}Mn activity had fully decayed.

Reactor power, irradiation time, and length of time waited before specific foil counting were optimized to reduce counter deadtime losses associated with high count rate, but without sacrificing statistical accuracy. In each case, sufficient counts were accumulated to ensure a statistical counting error of less than 0.5%.

6.3 Results and Discussions

Specific foil activity results, activity ratios relative to the thermal reference location, and the Westcott spectral parameters derived from these ratios are shown in Tables 11, 12 and 13. The detailed neutron temperature and epithermal index measurements in the central cells, between the thorium and natural UO_2 assemblies in adjacent rods, are shown in Figs. 19 and 20.

As expected, the neutron spectrum is much harder in the thorium fuel; both the epithermal index and neutron temperature are substantially higher than in equivalent 19-element natural UO_2. Also, since the 28 element natural UO_2 driver lattice is undermoderated at this pitch, the eight, 19-element UO_2 fuel assemblies surrounding the central rod site are perturbed and the spectrum is slightly harder than in the same fuel at the center of the core. The neutron spectrum is appreciably softer at the bundle ends where the thermal flux peaks, particularly in the thorium fuel.

Errors in individual foil activities were typically $\leq \pm 0.5\%$, based on counting reproducibility. The alloy content of the foils, determined by intercalibration, was accurate to about $\pm 0.7\%$. Thus the errors in the activity ratio results relative to the thermal reference location were approximately $\pm 1.2\%$. Resultant errors in the epithermal index, r, were typically $\sim \pm 1.5\%$; errors in the neutron temperatures are included in the tables of results.

7. SUMMARY

Detailed experiments have been performed in a mock-up power reactor lattice to determine detailed physics cell parameters and core perturbation effects associated with the substitution of 19-element $^{235}UO_2$ enriched ThO_2 fuel in a natural UO_2 core. Measurements were made at a square lattice pitch of 22.86 cm with D_2O coolant.

Core reactivity effects were determined as changes in critical moderator level for three configurations of thoria and natural UO_2 bundle substitutions at the central lattice site. In each case, the D_2O to air void effect was also determined. Macroscopic flux perturbation effects in the core for the two-bundle thorium configuration simulating the power reactor irradiation were measured by copper foil activation.

Detailed foil activation fine structure measurements were made in the central cells within fuel bundles, at calandria tube surfaces and in the moderator. Thermal and epithermal neutron energy spectrum information was inferred from relative Lu/Mn and In/Mn activity ratios, and expressed as the Westcott indices r and T_n.

The results demonstrate that the thoria fuel is a substantial absorber and indicate the extent of flux perturbation and spectral hardening in the central fuel rod and surrounding lattice. Calculated flux distributions agree reasonably well with experiment.

8. ACKNOWLEDGEMENTS

The author wishes to thank the many people associated with the experiments and production of the report, in particular to P.D.J. Ferrigan, E.J. Pleau and D.J. Roberts who helped perform the experiments, D.A. Kettner who assembled the measurement bundles, Mrs. D.E. Goldberg who prepared many of the drawings and helped analyze the data, Mrs. N. Yeatman who typed the manuscript, and H. Tamm (Whiteshell Nuclear Research Laboratory) who provided the fuel.

9. REFERENCES

1. E. Critoph. The Thorium Fuel Cycle in Water-Moderated Reactor Systems. Atomic Energy of Canada Limited, Report AECL-5705 (1977).

2. M.F. Duret. Introducing Advanced Nuclear Fuel Cycles in Canada. Atomic Energy of Canada Limited, Report AECL-6202 (1978).

3. E. Critoph, S. Banerjee, F.W. Barclay, D. Hamel, M.S. Milgram and J.I. Veeder. Prospects for Self-sufficient Equilibrium Thorium Cycles in CANDU Reactors. Atomic Energy of Canada Limited, Report AECL-5501 (1976).

4. S.R. Hatcher, S. Banerjee, A.D. Lane, H. Tamm and J.I. Veeder. Thorium Cycle in Heavy Water Moderated Pressure Tube (CANDU) Reactors. Atomic Energy of Canada Limited, Report AECL-5398 (1976).

5. H. Tamm and D. Hamel, unpublished Atomic Energy of Canada Limited report (1977).

6. C.H. Westcott. Effective Cross Section Values for Well Moderated Thermal Reactor Spectra. Atomic Energy of Canada Limited, Report AECL-1101 (1964).

7. R.T. Jones. Measurement of a Relative Conversion Ratio in 19-Element ThO_2-UO_2 Fuel. Atomic Energy of Canada Limited, Report AECL-5825 (1977).

8. K.J. Serdula and R.E. Green. Lattice Measurements with 28-element Natural UO_2 Fuel Assemblies - Part II: Relative Total Neutron Densities and Hyperfine Activity Distributions in a Lattice Cell. Atomic Energy of Canada Limited, Report AECL-2772 (1967).

9. R.E. Green and C.B. Bigham. Lattice Parameter Measurements in ZED-2. Proc. IAEA Symp. Experimental and Critical Experiments, Amsterdam (1963), II, 457-477 (1964).

10. D.M. Amundrud, private communication (1978).

11. G.J. Phillips and J. Griffiths. LATREP User's Manual. Atomic Energy of Canada Limited, Report AECL-3857 (1971).

12. A.P. Olson. PERIGEE Computer Code for Reactor Simulation in 3D, Using 1 or 2 Neutron Velocity Groups. Atomic Energy of Canada Limited, Report AECL-1901 (1964).

13. A. Okazaki and M.H.M. Roshd. Flux Measurements in the Pickering Unit 2 Reactor. Atomic Energy of Canada Limited, Report AECL-4131 (1972).

14. N.A. Keller, private communication (1979).

15. M.H.M. Roshd and H.C. Chow. The Analysis of Flux Peaking at Nuclear Fuel Bundle Ends Using PEAKAN. Atomic Energy of Canada Limited, Report AECL-6174 (1978).

16. D.M. O'Shea and L.C. Noderer. Integral Transport Method for Burnup in Heterogeneous Assemblies. Trans. Amer. Nucl. Soc. 10, 303 (1967).

17. C.B. Bigham, B.G. Chidley and R.B. Turner. Experimental Effective Fission Cross Sections and Neutron Spectra in a Uranium Fuel Rod. Part II. CANDU-Type Uranium Oxide Clusters. Atomic Energy of Canada Limited, Report AECL-1350 (1961).

18. C.B. Bigham and P.R. Tunnicliffe. Experimental Effective Fission Cross Sections and Neutron Spectra in a Uranium Fuel Rod. Part I: NRX Uranium Metal Rods. Atomic Energy of Canada Limited, Report AECL-1186 (1961).

19. G.C. Hanna. The Neutron Flux Perturbation Due to an Absorbing Foil: A Comparison of Theories and Experiment. Nuc. Sci. and Eng. 15, 325 (1963).

20. W.H. Walker, C.H. Westcott and T.K. Alexander. Measurement of Radiative Capture Resonance Integrals in a Thermal Reactor Spectrum, and the Thermal Cross Section of Pu-240. Can. J. Phys. 38, 57 (1960).

21. Canada's NRU Reactor. Atomic Energy of Canada Limited, Report AECL-484 (1957).

Table 1: MEASURED CRITICAL HEIGHT DATA

Core Description	Central Rod Coolant	Moderator Temp. (°C)	Moderator Purity (wt.%)	Critical Height (cm)
1. Reference Core: (Fig. 1) D_2O cooled	D_2O	19.94	99.631	231.488
2. As above	Air	19.98	99.631	231.037
3. Reference core	D_2O	20.50	99.621	232.675
4. Reference core + 5 thoria bundles in central rod	D_2O	20.47	99.621	241.224
5. As above	Air	20.62	99.621	241.080
6. Reference core	D_2O	20.50	99.621	232.675
7. Reference core + 2 thoria bundles in central rod	D_2O	20.57	99.621	238.420
8. Reference core	D_2O	19.94	99.631	231.488
9. Reference core + 2 thoria bundles in central rod	Air	20.06	99.631	236.985
10. Reference core	D_2O	20.56	99.634	231.677
11. Reference core + 1 thorium bundle in central rod	D_2O	20.91	99.634	234.450
12. Reference core	D_2O	20.56	99.635	231.535
13. 53 rods, 28-element UO_2 (D_2O cooled) plus 24 ZEEP rods	D_2O	20.04	99.636	249.771

TABLE 2: NORMALIZED CENTRAL CELL COPPER ACTIVITIES: 19-ELEMENT NATURAL UO_2 AT CORE CENTER

LOCATION	RADIUS (cm)	NORMALIZED ACTIVITY
Fuel (KO)	0.0	1.000
Fuel (KO)	1.651	1.090
Fuel (KO)	3.180	1.327
Fuel (KO)	3.180	1.335
Sheath (KO)	0.0	1.033
Sheath (KO)	1.651	1.128
Sheath (KO)	3.180	1.379
Sheath (KO)	3.180	1.383
Cal. Tube (KO):W	5.22	1.798
Cal. Tube (KO):S	5.22	1.800
Mod:N	5.33	1.815
Mod:N	6.22	1.993
Mod:N	7.22	1.129
Mod:N	8.22	2.229
Mod:N	9.22	2.308
Mod:N	10.22	2.335
Mod:N	11.43	2.358
Mod:N	12.22	2.348
Mod:N	13.22	2.306
Mod:N	14.22	2.235
Mod:N	14.72	2.172
Mod:NE	5.40	1.851
Mod:NE	6.22	2.004
Mod:NE	7.22	2.165
Mod:NE	8.22	2.269
Mod:NE	9.22	2.357

LOCATION	RADIUS (cm)	NORMALIZED ACTIVITY
Mod:NE	10.22	2.422
Mod:NE	11.22	2.478
Mod:NE	12.22	2.506
Mod:NE	13.22	2.538
Mod:NE	14.22	2.539
Mod:NE	15.22	2.555
Mod:NE	16.16	2.538
Mod:NE	17.22	2.544
Mod:NE	18.22	2.511
Mod:NE	19.22	2.509
Mod:NE	20.22	2.466
Mod:NE	21.22	2.407
Mod.EW	11.60	2.385
Mod:EW	12.11	2.430
Mod:EW	12.91	2.501
Mod:EW	13.95	2.525
Mod:EW	15.19	2.564
Cell Edge (K1E)	11.43	2.363
Cell Edge (K1W)	11.43	2.344
Cell Corner (KL1W)	16.16	2.574
Cal. Tube (K2E):W	17.64	1.750
Fuel (K2E)	19.68	1.311
Fuel (K2E)	21.21	1.053
Fuel (K2E)	22.86	0.966
Fuel (K2E)	26.04	1.260

TABLE 3: NORMALIZED CENTRAL CELL COPPER ACTIVITIES: TWO ThO_2-UO_2 BUNDLES REPLACING UO_2 AT CORE CENTER

LOCATION	RADIUS (cm)	NORMALIZED ACTIVITY
Fuel (KO)(ThO_2-UO_2)	0.0	1.000
Fuel (KO)(ThO_2-UO_2)	1.651	1.156
Fuel (KO)(ThO_2-UO_2)	1.651	1.163
Fuel (KO)(ThO_2-UO_2)	3.180	1.739
Fuel (KO)(ThO_2-UO_2)	3.180	1.719
Sheath (KO)	0.0	1.033
Sheath (KO)	1.651	1.209
Sheath (KO)	1.651	1.215
Sheath (KO)	3.180	1.834
Sheath (KO)	3.180	1.841
Cal. Tube (KO):S	5.22	2.821
Cal. Tube (KO):W	5.22	2.836
Mod:N	5.33	2.862
Mod:N	6.22	3.250
Mod:N	7.22	3.568
Mod:N	8.22	3.740
Mod:N	9.22	3.983
Mod:N	10.22	4.106
Mod:N	11.43	4.180
Mod:N	12.22	4.174
Mod:N	13.22	4.137
Mod:N	14.22	4.044
Mod:N	14.72	3.990
Mod:NE	5.40	2.866
Mod:NE	6.22	3.250
Mod:NE	7.22	3.611
Mod:NE	8.22	3.857
Mod:NE	9.22	4.078
Mod:NE	10.22	4.265
Mod:NE	11.22	4.372
Mod:NE	12.22	4.463
Mod:NE	13.22	4.538
Mod:NE	14.22	4.600
Mod:NE	15.22	4.627
Mod:NE	16.16	4.641
Mod:NE	17.22	4.680
Mod:NE	18.22	4.632
Mod:NE	19.22	4.614
Mod:NE	20.22	4.559
Mod:NE	21.22	4.453
Mod:EW	11.60	4.185
Mod:EW	12.11	4.305
Mod:EW	12.94	4.426
Mod:EW	13.95	4.533
Mod:EW	15.19	4.616
Cell Edge (K1E)	11.43	4.180
Cell Edge (K1W)	11.43	4.184
Cell Corner (KL1W)	16.16	4.638
Cal. Tube (K2E):W	17.64	3.224
Fuel (K2E)	19.68	2.472
Fuel (K2E)	21.21	1.977
Fuel (K2E)	22.86	1.830
Fuel (K2E)	26.04	2.367

TABLE 4: NORMALIZED CENTRAL CELL COPPER ACTIVITIES: FIVE ThO_2-UO_2 BUNDLES REPLACING UO_2 AT CORE CENTER

LOCATION	RADIUS (cm)	NORMALIZED ACTIVITY
Fuel (KO)(ThO_2-UO_2)	0.0	1.000
Fuel (KO)(ThO_2-UO_2)	1.651	1.156
Fuel (KO)(ThO_2-UO_2)	1.651	1.172
Fuel (KO)(ThO_2-UO_2)	3.180	1.735
Fuel (KO)(ThO_2-UO_2)	3.180	1.726
Cal. Tube (KO):S	5.22	3.057
Cal. Tube (KO):SW	5.22	3.059
Mod:N	5.32	2.960
Mod:N	6.22	3.326
Mod:N	7.22	3.627
Mod:N	8.22	3.943
Mod:N	9.22	4.097
Mod:N	10.22	4.209
Mod:N	11.43	4.267
Mod:N	12.22	4.276
Mod:N	13.22	4.239
Mod:N	14.22	4.166
Mod:N	14.72	4.057
Mod:NE	5.33	3.069
Mod:NE	6.22	3.365
Mod:NE	7.22	3.710
Mod:NE	8.22	4.000

LOCATION	RADIUS (cm)	NORMALIZED ACTIVITY
Mod:NE	9.22	4.198
Mod:NE	10.22	4.337
Mod:NE	11.22	4.483
Mod:NE	12.22	4.402
Mod:NE	13.22	4.654
Mod:NE	14.22	4.726
Mod:NE	15.22	4.729
Mod:NE	16.16	4.740
Mod:NE	17.22	4.734
Mod:NE	18.22	4.710
Mod:NE	19.22	4.677
Mod:NE	20.22	4.631
Mod:NE	21.22	4.549
Mod:E-W	11.60	4.333
Mod:E-W	12.11	4.433
Mod:E-W	12.91	4.565
Mod:E-W	13.95	4.673
Mod:E-W	15.19	4.747
Cell Edge (K1E)	11.43	4.156
Cell Corner (KL1W)	16.16	4.690
Cal. Tube (K2E):W	17.64	3.212

TABLE 5: NORMALIZED CORE Cu ACTIVITIES: 19-ELEMENT NATURAL UO_2 AT CORE CENTER

ELEVATION (cm)	LOCATION AND RADIUS (cm)																	
	K9W	K7W	K5W	K3W	K1W	KL1W	KO (WEST)	KO FUEL					K1E	K2E (WEST)	K2E FUEL			
	102.87	80.01	57.15	34.29	11.43	16.16	5.22	3.18	1.65	0.0	1.65	3.18	11.43	17.64	19.68	21.21	22.86	26.04
215	0.494						0.571						0.720	0.562				
205	0.655						0.775						1.012	0.771				
195	0.813						0.977						1.286	0.967				
187.6	(0.911)						(1.125)	(0.831)	(0.682)	(0.626)		(0.835)	(1.470)	(1.094)				
185	0.956						1.179						1.539	1.152				
175	1.082						1.362						1.777	1.326				
165	1.203						1.560						1.999	1.521				
155	1.310						1.650						2.166	1.614				
145	1.392	1.340	1.545	1.927	2.287	2.488	1.747						2.290	1.700				
139.2	(1.436)						(1.798)	1.327	1.090	1.000	(1.09)	1.335	(2.363)	(1.750)	1.311	1.053	0.966	1.260
135	1.463	1.395	1.612	2.022	2.385	2.618	1.829						2.390	1.780				
125	1.494						1.894						2.482	1.835				
115	1.526						1.986						2.564	1.932				
105	1.529						1.912						2.510	1.872				
95	1.517						1.855						2.457	1.822				
85	1.468						1.796						2.374	1.768				
75	1.395						1.729						2.264	1.693				
65	1.310						1.666						2.141	1.629				
55	1.204						1.486						1.924	1.446				
45	1.077						1.313						1.711	1.290				
35	0.954						1.151						1.483	1.117				
25	0.801						0.999						1.279	0.969				

Figures in parentheses have been interpolated.

KO (WEST) and K2E (WEST) refer to activities on WEST sides of calandria tubes.

TABLE 6: NORMALIZED CORE Cu ACTIVITIES: 2 ThO_2-UO_2 BUNDLES REPLACING NATURAL UO_2 AT CORE CENTER

ELE-ATION (cm)	LOCATION AND RADIUS (cm)																	
	K9W	K7W	K5W	K3W	K1W	KL1W	K0 (WEST)	K0 FUEL					K1E	K2E (WEST)	K2E FUEL			
	102.87	80.01	57.15	34.29	11.43	16.16	5.22	3.18	1.65	0.0	1.65	3.18	11.43	17.64	19.68	21.21	22.86	26.04
215	1.093						1.251						1.610	1.230				
205	1.392						1.615						2.137	1.612				
195	1.677						1.977						2.598	1.956				
187.6	(1.875)						(2.241)	1.703	1.367	1.263		1.692	(2.943)	(2.195)				
185	1.965						2.334						3.064	2.279				
175	2.186						2.631						3.471	2.578				
165	2.419						2.898						3.765	2.897				
155	2.591						2.692						3.960	3.048				
145	2.738	2.609	3.004	3.677	4.111	4.562	2.770						4.073	3.184				
139.2	(2.836)						(2.837)	1.739	1.156	1.000	1.163	1.719	(4.178)	(3.224)	2.472	1.977	1.830	2.367
135	2.895	2.709	3.088	3.825	4.258	4.720	2.886						4.254	3.281				
125	2.950						3.000						4.390	3.392				
115	2.994						3.190						4.484	3.577				
105	3.002						3.018						4.411	3.421				
95	2.971						2.931						4.316	3.335				
85	2.889						2.845						4.164	3.224				
75	2.749						2.730						4.013	3.100				
65	2.576						2.794						3.86	3.008				
55	2.383						2.721						3.606	2.682				
45	2.134						2.455						3.197	2.395				
35	1.873						2.154						2.807	2.071				
25	1.593						1.872						2.408	1.803				

Figures in parentheses have been interpolated.

K0 (WEST) and K2E (WEST) refer to activities on WEST sides of calandria tubes.

TABLE 7: MODERATOR FLUX PERTURBATION FACTOR DISTRIBUTION IN CENTRAL CELL

LOCATION	RADIUS (cm)	F(r,z)
Mod:N	5.33	0.798
Mod:N	6.22	0.825
Mod:N	7.22	0.848
Mod:N	8.22	0.849
Mod:N	9.22	0.853
Mod:N	10.22	0.890
Mod:N	11.43	0.897
Mod:N	12.22	0.890
Mod:N	13.22	0.908
Mod:N	14.22	0.916
Mod:N	14.72	0.930
Mod:NE	5.40	0.783
Mod:NE	6.22	0.821
Mod:NE	7.22	0.844
Mod:NE	8.22	0.860
Mod:NE	9.22	0.875
Mod:NE	10.22	0.891
Mod:NE	11.22	0.893

LOCATION	RADIUS (cm)	F(r,z)
Mod:NE	12.22	0.901
Mod:NE	13.22	0.905
Mod:NE	14.22	0.917
Mod:NE	15.22	0.916
Mod:NE	16.16	0.925
Mod:NE	17.22	0.931
Mod:NE	18.22	0.933
Mod:NE	19.22	0.931
Mod:NE	20.22	0.936
Mod:NE	21.22	0.937
Mod:EW	11.43	0.897
Mod:EW	11.60	0.888
Mod:EW	12.11	0.897
Mod:EW	12.91	0.890
Mod:EW	13.95	0.908
Mod:EW	15.19	0.911
Mod:EW	16.16	0.925

TABLE 8: CORE FLUX PERTURBATION FACTORS

ELEVATION (cm)	LOCATION AND RADIUS (cm)																
	K9W 102.87	K7W 80.01	K5W 57.15	K3W 34.29	K1W 11.43	KL1W 16.16	KO (WEST) 5.22	KO FUEL 3.18	1.65	0.0	1.65	3.18	K1E 11.43	K2E (WEST) 17.64	K2E FUEL 19.68	21.21	22.86	26.04
215	1.000						0.990						1.010	0.988				
205	1.000						0.981						0.998	0.984				
195	1.000						0.981						0.979	0.981				
187.6	1.000						0.967	0.996	0.975	0.981		0.985	0.972	0.974				
185	1.000						0.963						0.968	0.962				
175	1.000						0.955						0.966	0.961				
165	1.000						0.923						0.936	0.947				
155	1.000						0.825						0.924	0.954				
145	1.000	0.990	0.988	0.970	0.914	0.932	0.806						0.904	0.952				
139.2	1.000	(0.985)	(0.978)	(0.963)	(0.908)	(0.922)	0.798	0.663	0.536	0.506	0.539	0.652	0.895	0.933	0.955	0.950	0.958	0.950
135	1.000	0.981	0.968	0.956	0.902	0.911	0.797						0.899	0.931				
125	1.000						0.802						0.895	0.935				
115	1.000						0.818						0.891	0.943				
105	1.000						0.803						0.895	0.930				
95	1.000						0.806						0.897	0.934				
85	1.000						0.804						0.891	0.926				
75	1.000						0.811						0.899	0.929				
65	1.000						0.852						0.918	0.939				
55	1.000						0.925						0.947	0.937				
45	1.000						0.943						0.943	0.937				
35	1.000						0.952						0.963	0.944				
25	1.000						0.942						0.946	0.935				

Figures in parentheses have been interpolated
KO (WEST) and K2E (WEST) refer to activities on WEST sides of calandria tubes.

TABLE 9

FOIL ACTIVATION RESULTS AT FUEL STACK ENDS IN DEMOUNTABLE BUNDLES - THORIA BUNDLE ABUTTING NATURAL UO_2

FUEL TYPE	ELEMENT LOCATION	DISTANCE FROM * FUEL END (cm)	NORMALIZED ACTIVITY	FUEL TYPE	ELEMENT LOCATION	DISTANCE FROM * FUEL END (cm)	NORMALIZED ACTIVITY
Thoria	Outer	0.00 (162.4)	1.483	Thoria	Middle	0.00 (162.4)	1.847
		2.00 (160.4)	1.140			1.80 (160.6)	1.217
		3.90 (158.5)	1.069			3.70 (158.7)	1.127
		5.90 (156.5)	1.044			23.20 (139.2)	1.000
		7.80 (154.6)	1.032				
		11.70 (150.7)	1.013	UO_2	Outer	0.00 (165.3)	1.114
		15.60 (146.8)	1.004			2.10 (167.4)	1.016
		19.50 (142.9)	1.004			4.20 (169.5)	1.002
		23.20 (139.2)	1.000			6.20 (171.5)	1.000
						22.30 (187.6)	1.000

*Core elevations in parentheses.

TABLE 10: COMPARISON OF CALCULATED AND MEASURED BUNDLE END FLUX PEAKING FACTORS - THORIA BUNDLE ABUTTING NATURAL UO_2

Fuel Ring	Fuel Type	
	ThO_2	UO_2
OUTER	1.48 (1.50)	1.12 (1.11)
INTERMEDIATE	1.80 (1.90)	1.19
INNER	1.91	1.21

Experimental values in parentheses.

Table 11: NEUTRON SPECTRUM DATA: Two ThO_2-UO_2 BUNDLES REPLACING UO_2 AT CORE CENTER

LOCATION	ELEVATION (cm)	RADIUS (cm)	In	Mn	Lu	$\frac{(In/Mn)_x}{(In/Mn)_{Ref.}}$	$\frac{(Lu/Mn)_x}{(Lu/Mn)_{Ref.}}$	$r\sqrt{\frac{T_n}{T_o}}$	r	ΔT (1) (°C)
Fuel Rod Ko										
ThO_2-UO_2 - Pin 1	127.7	3.180	3.623	1.659	2.012	2.184	1.213	0.0728	0.0658	66.0 ± 4.8
- Pin 2	127.7	1.651	3.043	1.090	1.486	2.792	1.364	0.1128	0.0937	132.6 ± 9.2
- Pin 3	127.7	0.000	2.832	0.956	1.306	2.963	1.367	0.1246	0.1026	139.8 ± 10.2
Pin 4	127.7	1.651	3.050	1.096	1.469	2.783	1.340	0.1123	0.0942	123.7 ± 8.9
Pin 5	127.7	3.180	3.620	1.600	1.985	2.262	1.240	0.0778	0.0694	76.2 ± 5.4
Fuel Average	127.7		3.398	1.425	1.798	2.385	1.262	0.0897	0.0778	92.7 ± 6.6
ThO_2-UO_2 - Pin 2	162.5	1.651	3.287	1.650	1.987	1.992	1.204	0.0605	0.0551	60.4 ± 3.9
- Pin 3	162.5	0.000	3.167	1,549	1.895	2.045	1.224	0.0638	0.0576	67.3 ± 4.4
- Pin 5	162.5	3.180	3.661	1.961	2.310	1.867	1.177	0.0526	0.0485	50.9 ± 3.8
UO_2 - Pin 2	165.3	1.651	3.467	1.828	2.196	1.396	1.201	0.0544	0.0497	58.3 ± 3.6
- Pin 3	165.3	0.000	3.323	1.722	2.089	1.930	1.213	0.0565	0.0513	62.3 ± 4.4
- Pin 5	165.3	3.180	3.793	2.103	2.468	1.803	1.173	0.0486	0.0450	49.1 ± 3.5
UO_2 - Pin 1	189.7	3.180	2.680	1.470	1.757	1.823	1.195	0.0497	0.0456	55.6 ± 4.2
- Pin 2	189.7	1.651	2.341	1.181	1.447	1.982	1.226	0.0598	0.0540	67.0 ± 5.0
- Pin 3	189.7	0.000	2.233	1.096	1.374	2.038	1.254	0.0632	0.0563	76.4 ± 5.0
- Pin 5	189.7	3.180	2.646	1.470	1.704	1.800	1.159	0.0484	0.0451	44.9 ± 3.9
Fuel Average	189.7		2.539	1.359	1.622	1.868	1.194	0.0532	0.0487	56.9 ± 4.4
Fuel Rod K2E										
UO_2 - Pin 1	137.1	19.68	4.102	2.212	2.600	1.855	1.175	0.0518	0.0479	50.2 ± 3.9
- Pin 2	137.1	21.21	3.639	1.763	2.208	2.064	1.252	0.0649	0.0578	76.4 ± 4.8
- Pin 3	137.1	22.86	3.455	1.647	2.1[illegible]	2.098	1.276	0.0670	0.0591	84.4 ± 5.4
- Pin 5	137.1	26.04	4.043	2.149	2.524	1.881	1.174	0.0535	0.0495	50.2 ± 4.8
Fuel Average	137.1		3.903	2.021	2.426	1.932	1.201	0.0573	0.0521	60.3 ± 4.5
Calandria Tube KO(S)	125.0	5.22	4.742	2.672	2.978	1.775	1.114	0.0470	0.0447	31.4 ± 3.0
Calandria Tube K2W(E)	125.0	17.64	5.025	3.031	3.386	1.658	1.117	0.0396	0.0377	31.6 ± 2.9
Cell Edge K1W	125.0	11.43	6.085	3.869	4.176	1.573	1.079	0.0345	0.0334	20.5 ± 2.7
Cell Corner KLIW	125.0	16.16	6.534	4.351	4.607	1.502	1.059	0.0302	0.0295	14.6 ± 2.4
Reference Thermal Pit	137.1	150.3	1.000	1.000	1.000	1.000	1.000	8.3×10^{-5}	$T_{Ref} = 21.1°C$	

(1) $\Delta T = T_n - T_{Ref}$ $(T_{Ref} = T_{D2O})$

Table 12: NEUTRON SPECTRUM DATA: Five ThO_2-UO_2 BUNDLES REPLACING UO_2 AT CORE CENTER

LOCATION	ELEVATION (cm)	RADIUS (cm)	In	Mn	Lu	$\frac{(In/Mn)_x}{(In/Mn)_{Ref.}}$	$\frac{(Lu/Mn)_x}{(Lu/Mn)_{Ref.}}$	$r\sqrt{\frac{T_n}{T_o}}$	r	ΔT (1) (°C)
Fuel Rod Ko										
ThO_2-UO_2 - Pin 1	129.2	3.180	3.654	1.627	2.015	2.245	1.238	0.0767	0.0685	75.2 ± 5.0
- Pin 2	129.2	1.651	3.041	1.106	1.466	2.751	1.326	0.1101	0.0931	117.7 ± 9.2
- Pin 3	129.2	0.000	2.828	0.954	1.290	2.965	1.352	0.1248	0.1034	134.4 ± 12.9
- Pin 4	129.2	1.651	3.035	1.109	1.472	2.737	1.327	0.1092	0.0923	117.7 ± 9.5
- Pin 5	129.2	3.180	3.621	1.634	2.000	2.216	1.224	0.0748	0.0673	70.2 ± 5.0
Fuel Average	129.2		3.406	1.430	1.800	2.382	1.259	0.0890	0.0776	90.1 ± 6.8
Calandria Tube KO(S)	125.0	5.22	4.831	2.705	3.026	1.786	1.119	0.0477	0.0452	32.8 ± 2.1
Calandria Tube KO(SW)	125.0	5.22	4.781	2.662	3.029	1.796	1.138	0.0482	0.0453	38.6 ± 2.4
Calandria Tube K2E(W)	125.0	17.64	5.049	3.038	3.373	1.662	1.110	0.0399	0.0380	29.7 ± 1.9
Moderator - NE	129.5	9.22	6.110	3.932	4.215	1.554	1.072	0.0333	0.0323	18.4 ± 1.8
	129.5	13.22	6.569	4.337	4.601	1.515	1.061	0.0309	0.0302	15.2 ± 1.7
	129.5	17.22	6.549	4.429	4.718	1.478	1.065	0.0287	0.0279	16.5 ± 1.7
	129.5	21.22	6.439	4.295	4.558	1.499	1.061	0.0300	0.0292	15.4 ± 1.6
Moderator - N	129.5	8.22	5.778	3.621	3.931	1.596	1.086	0.0359	0.0346	22.4 ± 2.0
	129.5	11.22	6.148	3.992	4.259	1.540	1.067	0.0325	0.0316	17.0 ± 1.7
	129.5	14.22	6.014	3.852	4.192	1.562	1.088	0.0337	0.0325	23.1 ± 1.8
Cell Edge K1W	125.0	11.43	6.001	3.898	4.144	1.539	1.063	0.0325	0.0316	15.9 ± 1.8
Cell Corner KL1W	125.0	16.16	6.557	4.294	4.632	1.527	1.079	0.0316	0.0306	20.4 ± 1.8
	155.0	16.16	5.886	3.867	4.138	1.522	1.070	0.0314	0.0305	17.8 ± 2.6
Reference Thermal Pit	137.1	150.3	1.000	1.000	1.000	1.000	1.000	7.2×10^{-5} T_{Ref} = 20.17°C		

(1) $\Delta T = T_n - T_{Ref}$ $(T_{Ref} = T_{D_2O})$

Table 13: NEUTRON SPECTRUM DATA: NATURAL UO_2 AT CORE CENTER

LOCATION	ELEVATION (cm)	RADIUS (cm)	In	Mn	Lu	$\frac{(In/Mn)_x}{(In/Mn)_{Ref.}}$	$\frac{(Lu/Mn)_x}{(Lu/Mn)_{Ref.}}$	$r\sqrt{\frac{T_n}{T_o}}$	r	ΔT (°C) (1)
Fuel Rod Ko										
UO_2 - Pin 1	137.1	3.180	4.389	2.369	2.844	1.853	1.200	0.0516	0.0472	57.8 ± 3.0
- Pin 2	137.1	1.651	3.877	1.955	2.456	1.983	1.256	0.0597	0.0532	76.2 ± 3.8
- Pin 3	137.1	0.000	3.714	1.788	2.303	2.077	1.288	0.0657	0.0576	87.9 ± 3.8
- Pin 5	137.1	3.180	4.412	2.403	2.862	1.837	1.191	0.0506	0.0465	54.8 ± 2.3
Fuel Average	137.1		4.199	2.218	2.699	1.983	1.217	0.0546	0.0494	64.2 ± 3.1
Fuel Rod K2E										
UO_2 - Pin 1	137.1	19.68	4.302	2.309	2.795	1.863	1.210	0.0522	0.0475	60.8 ± 3.1
- Pin 2	137.1	21.21	3.789	1.862	2.355	2.035	1.265	0.0630	0.0559	79.9 ± 3.7
- Pin 3	137.1	22.86	3.606	1.721	2.175	2.095	1.264	0.0669	0.0592	80.8 ± 3.8
- Pin 5	137.1	26.04	4.217	2.222	2.676	1.898	1.204	0.0545	0.0497	59.5 ± 2.9
Fuel Average	137.1		4.077	2.109	2.586	1.933	1.226	0.0571	0.0515	67.5 ± 3.3
Calandria Tube K0(S)	125.0	5.22	5.487	3.335	3.738	1.645	1.121	0.0389	0.0369	32.8 ± 2.2
Calandria Tube K2W(E)	125.0	17.64	5.371	3.213	3.631	1.672	1.130	0.0405	0.0382	35.6 ± 2.6
Cell Edge K1W	125.0	11.43	6.622	4.281	4.610	1.547	1.077	0.0329	0.0318	19.9 ± 2.0
Cell Corner K1W	125.0	16.16	7.063	4.710	4.997	1.500	1.061	0.0300	0.0293	15.3 ± 2.2
	155.0	16.16	6.145	4.057	4.384	1.515	1.081	0.0309	0.0299	20.9 ± 2.0
Reference Thermal Pit	137.1	150.3	1.000	1.000	1.000	1.000	1.000	9.3×10^{-5}	T_{Ref} = 20.44°C	

(1) $\Delta T = T_n - T_{Ref}$ $(T_{Ref} = T_{D_2O})$

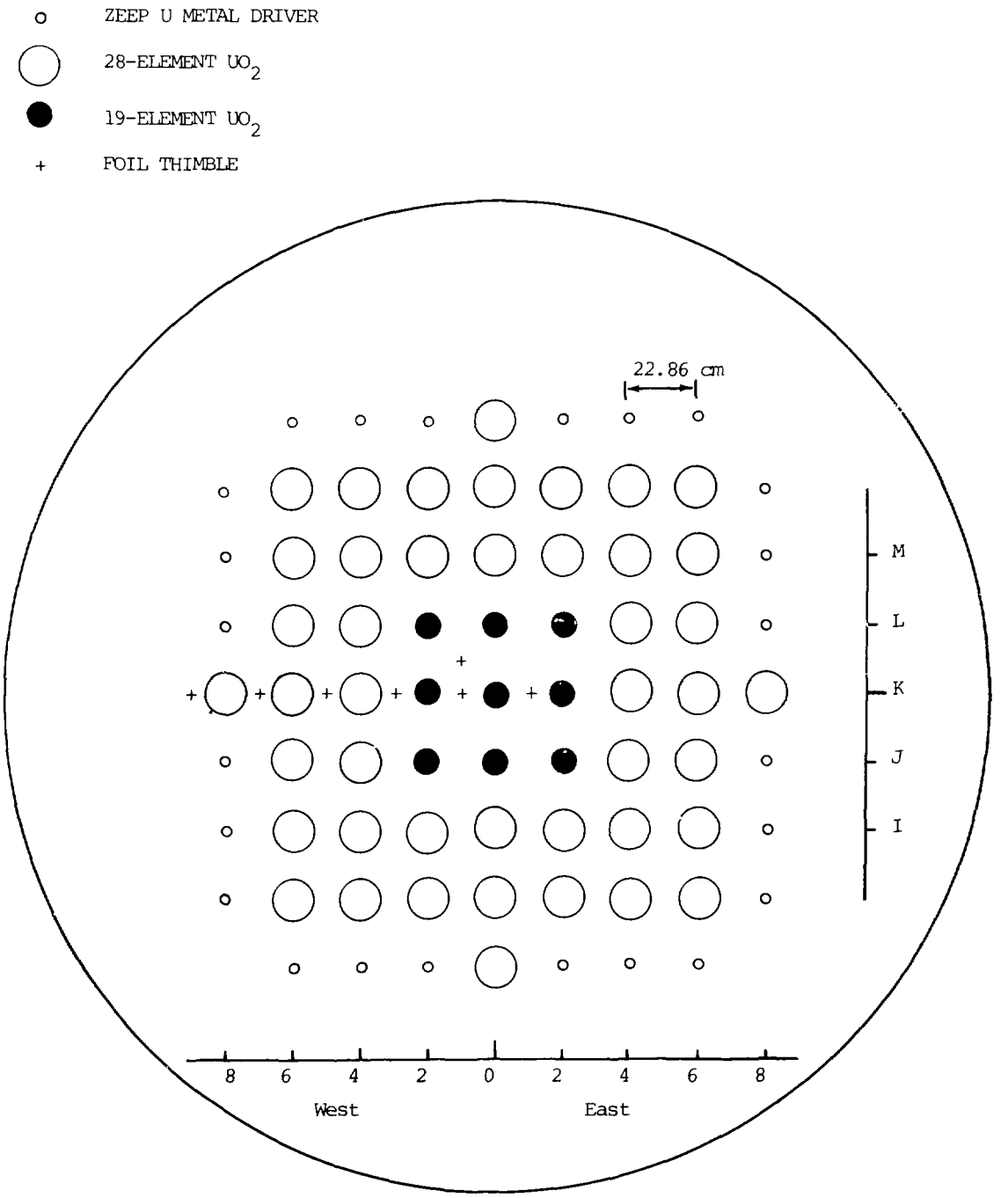

Figure 1: ZED-2 Reference Lattice

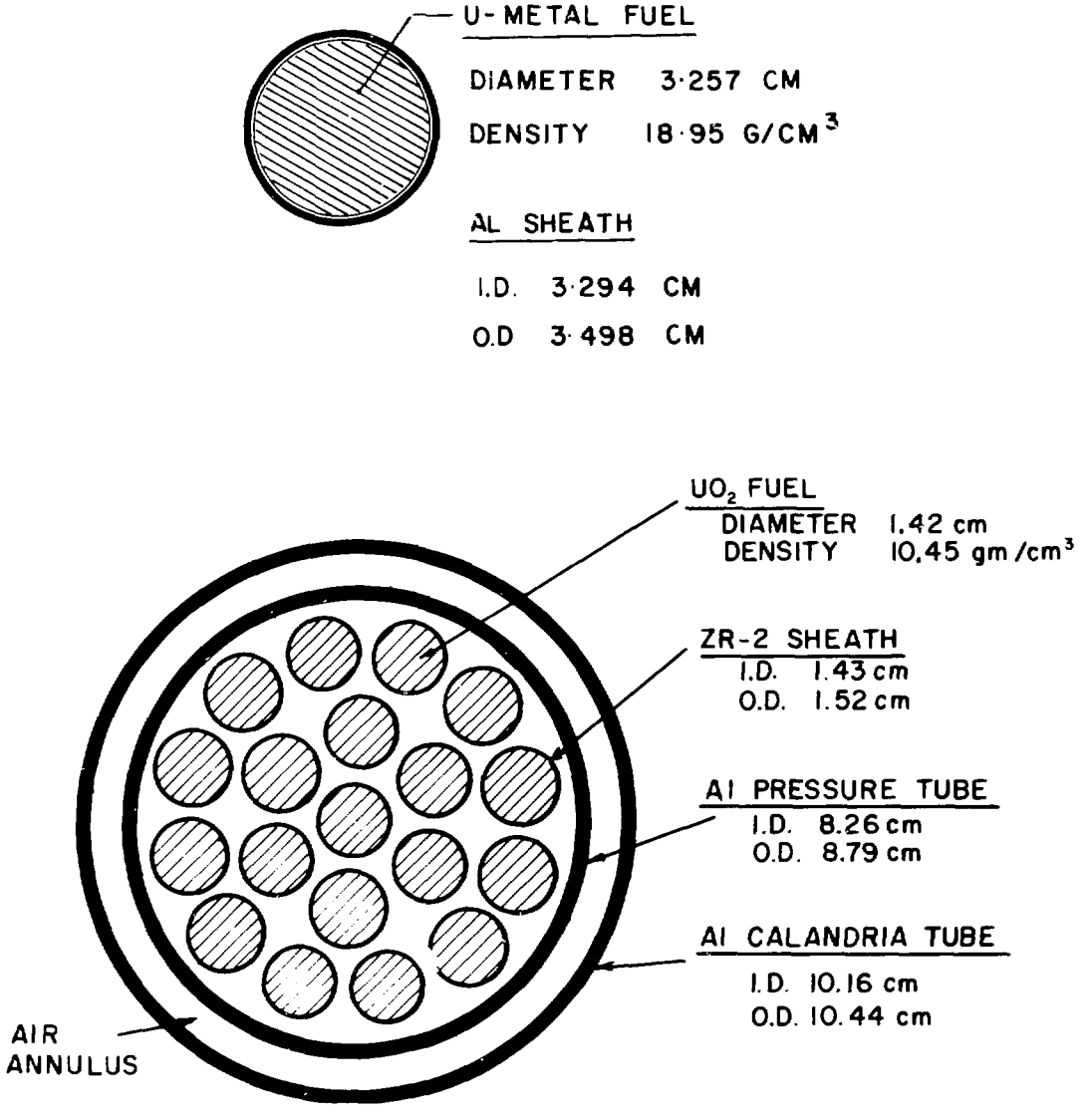

Figure 2: U-Metal ZEEP and 28-Element UO_2 Driver Fuel

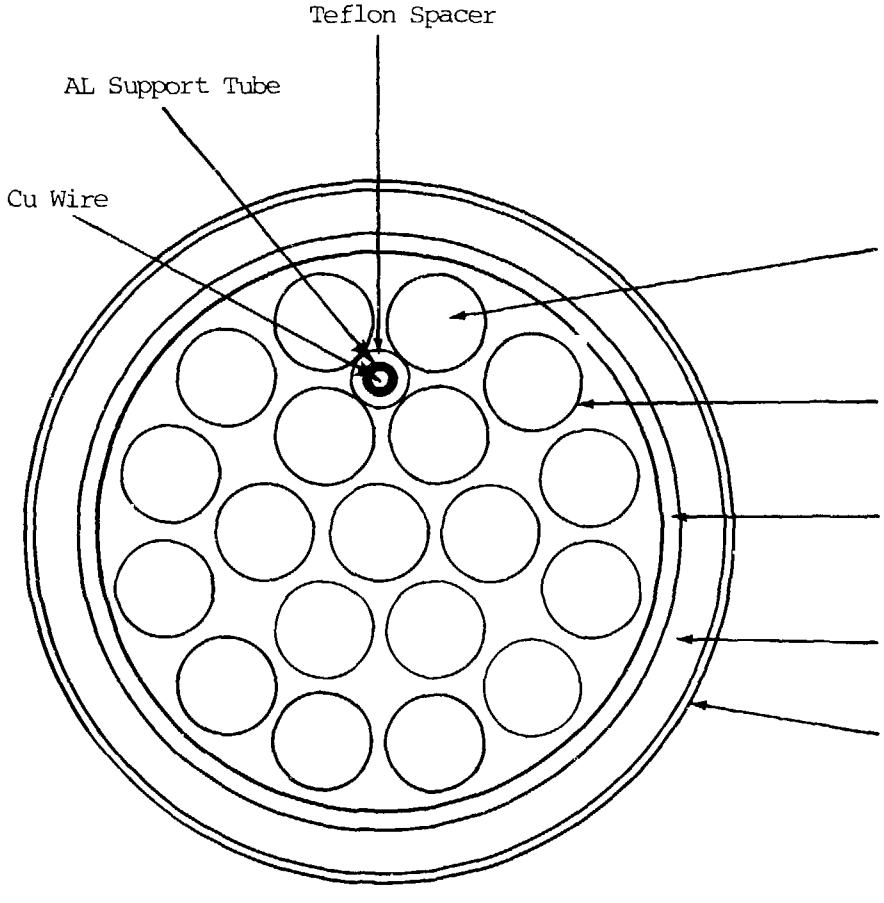

Figure 3: 19-Element UO_2 Fuel

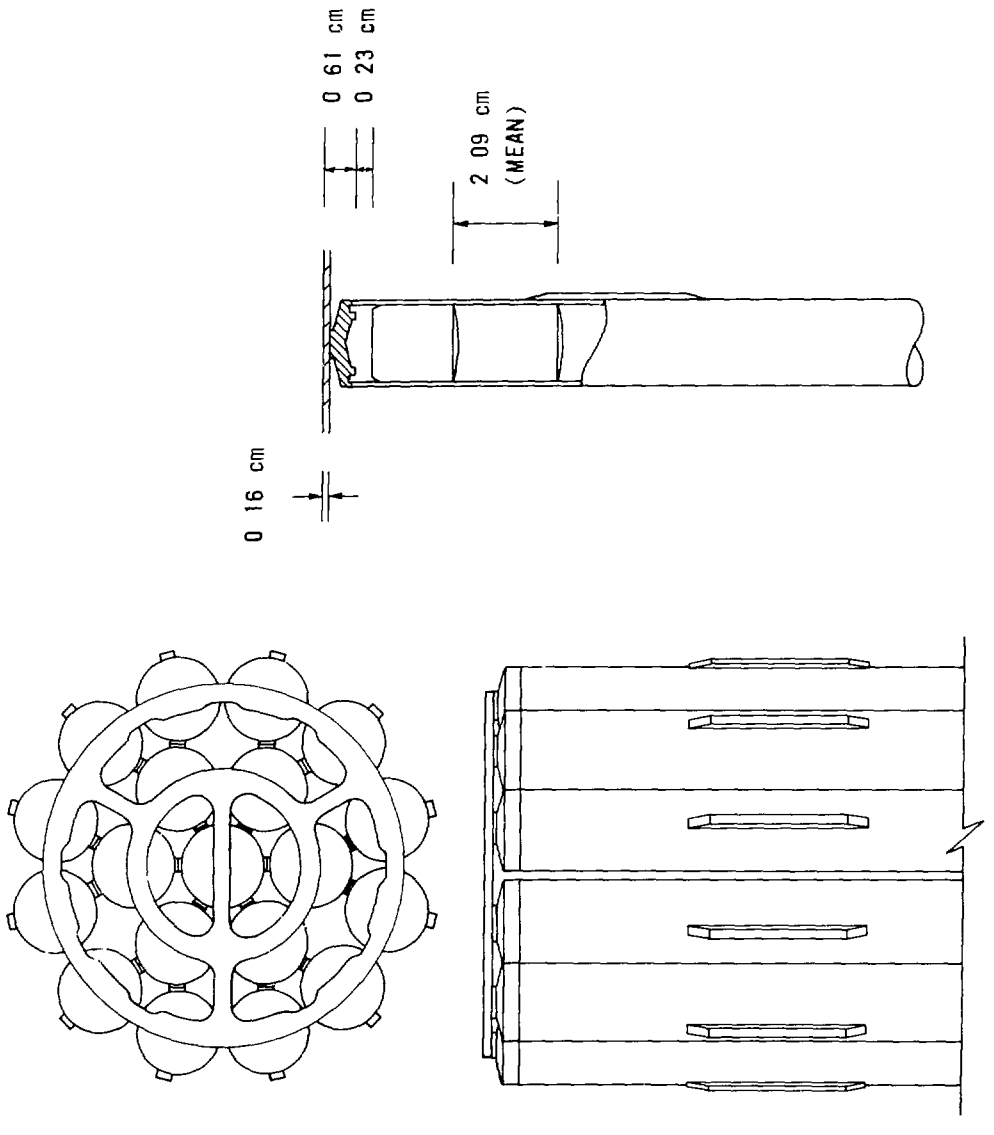

Figure 4: 19-Element Production Fuel Bundle End Region Detail

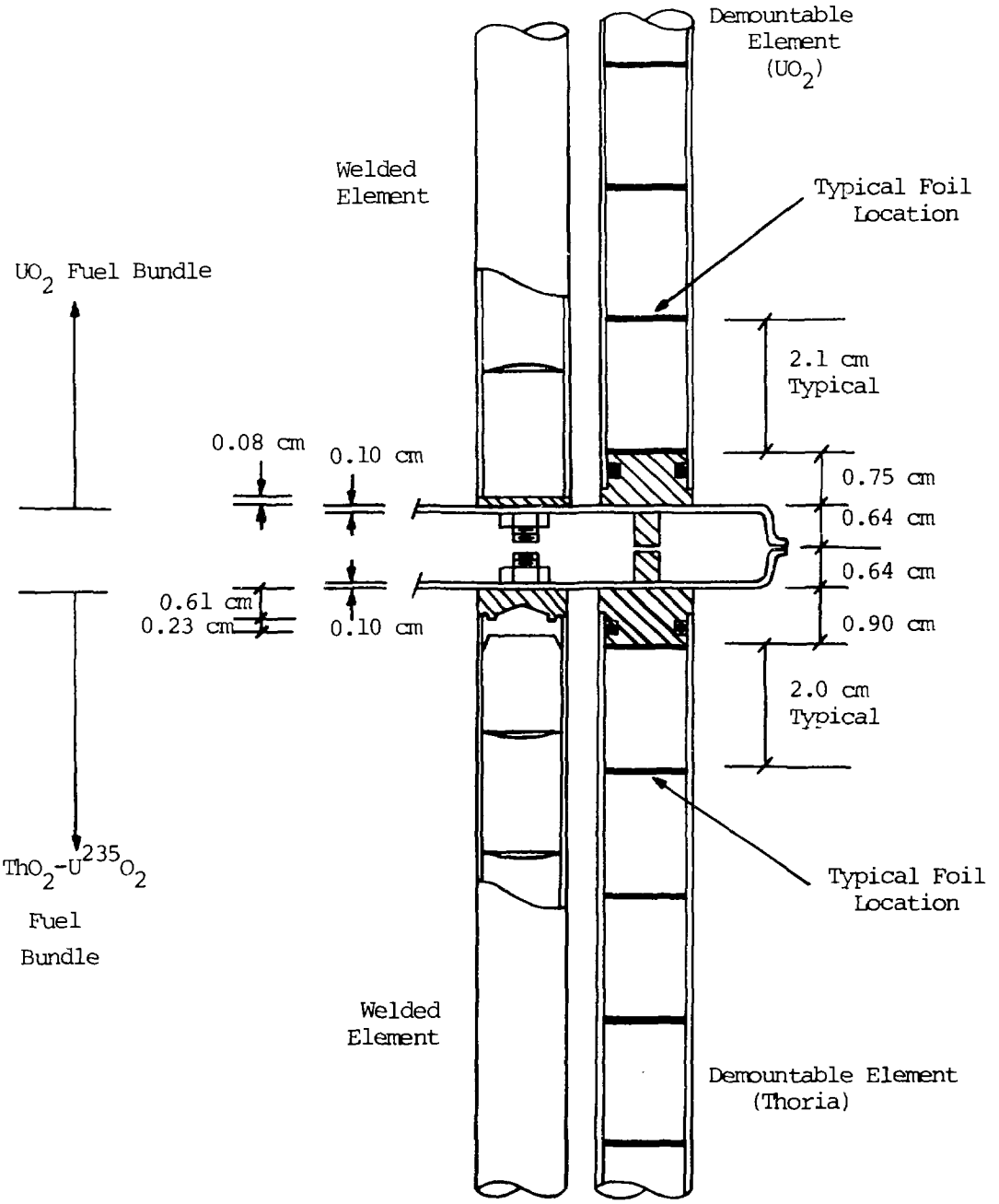

Figure 5: 19-Element Demountable Fuel Bundle End Region Detail

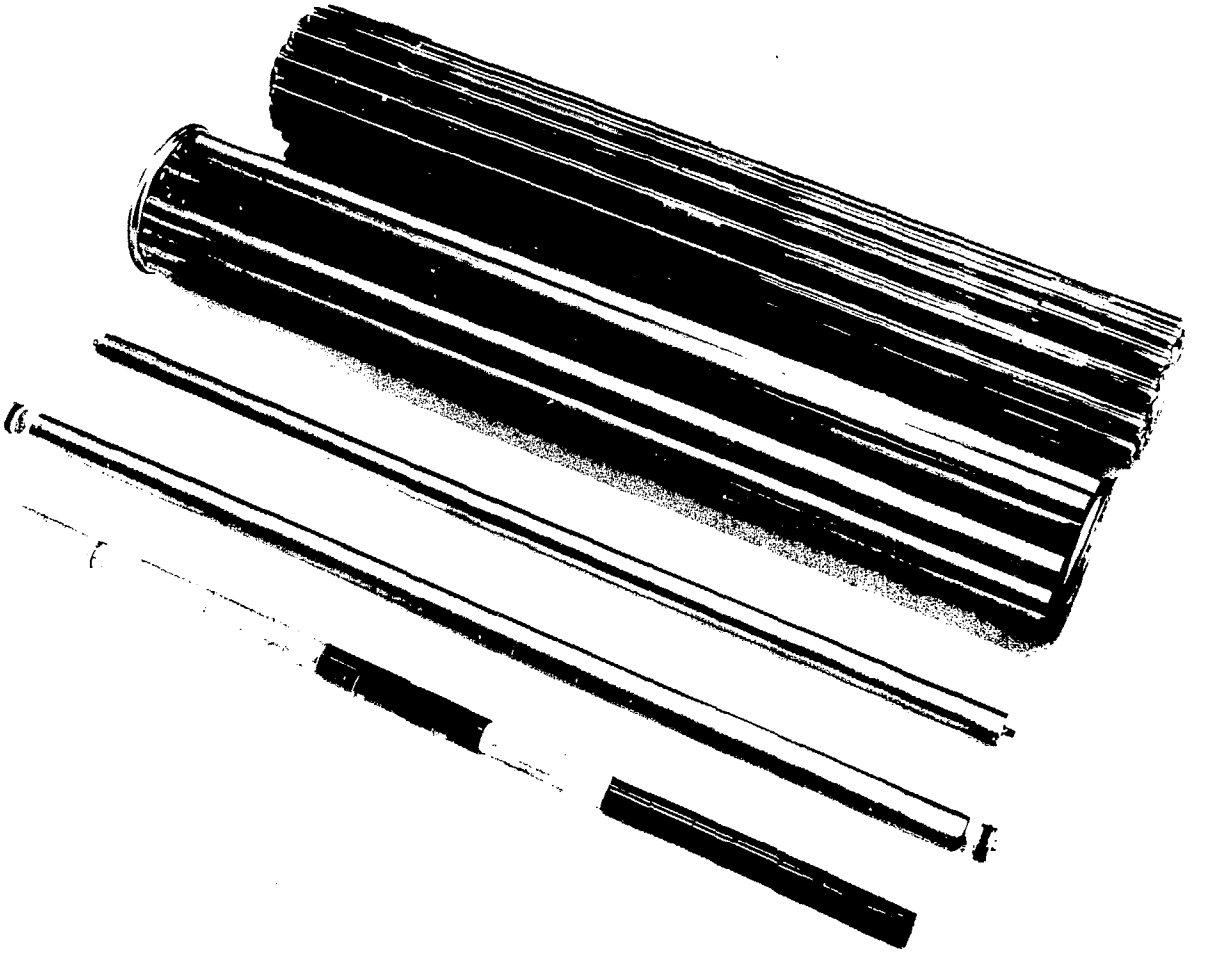

Figure 6: 19-Element Natural UO_2 Demountable Bundle

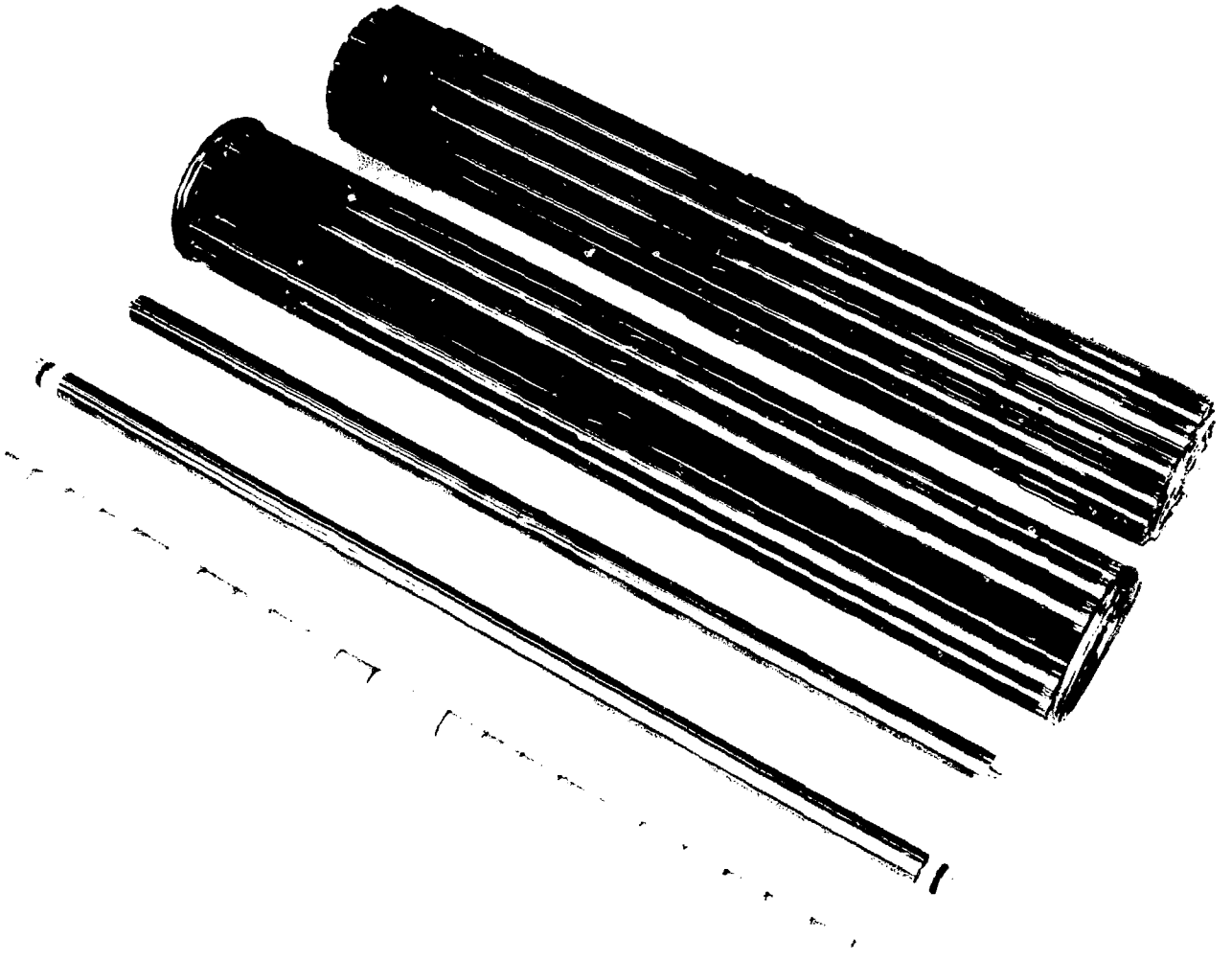

Figure 7: 19-Element ThO_2-UO_2 Demountable Fuel Bundle

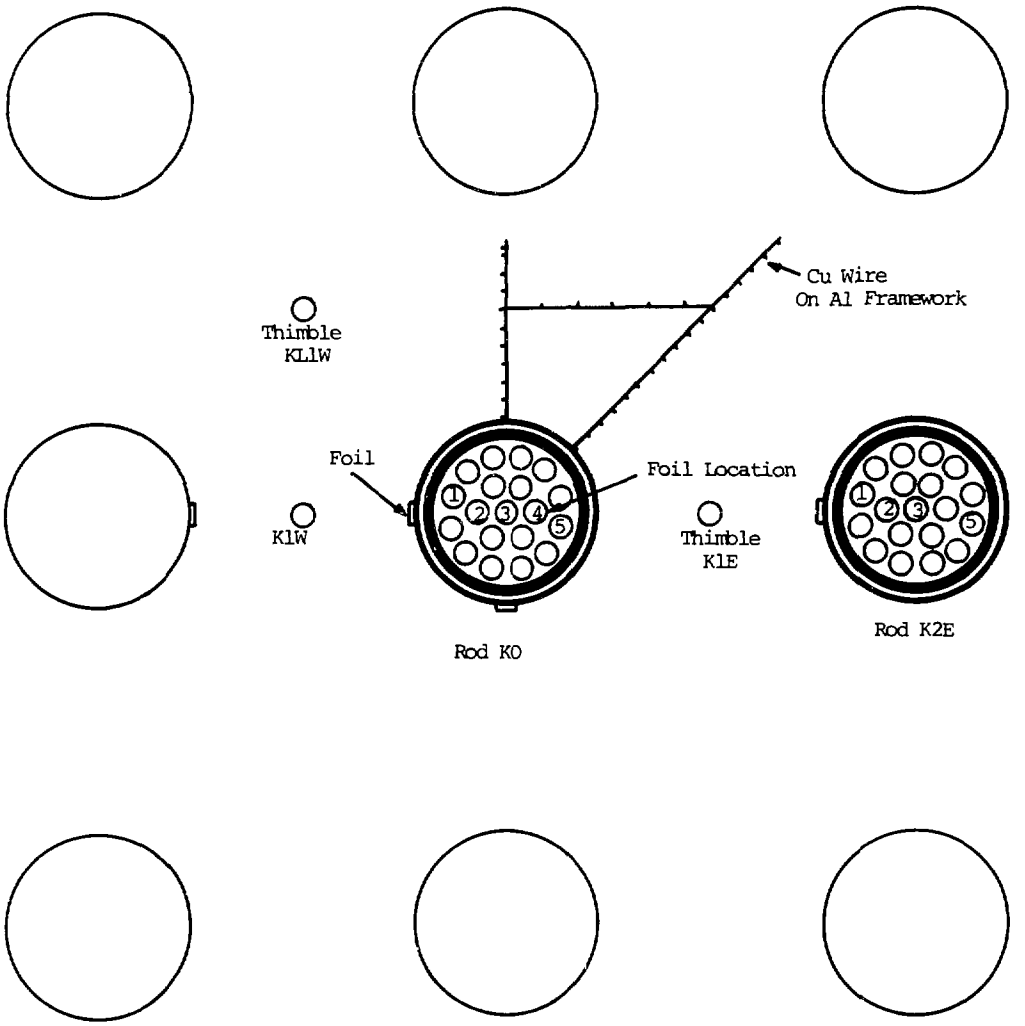

Figure 8: Detector Radial Measurement Locations in the Central Cell

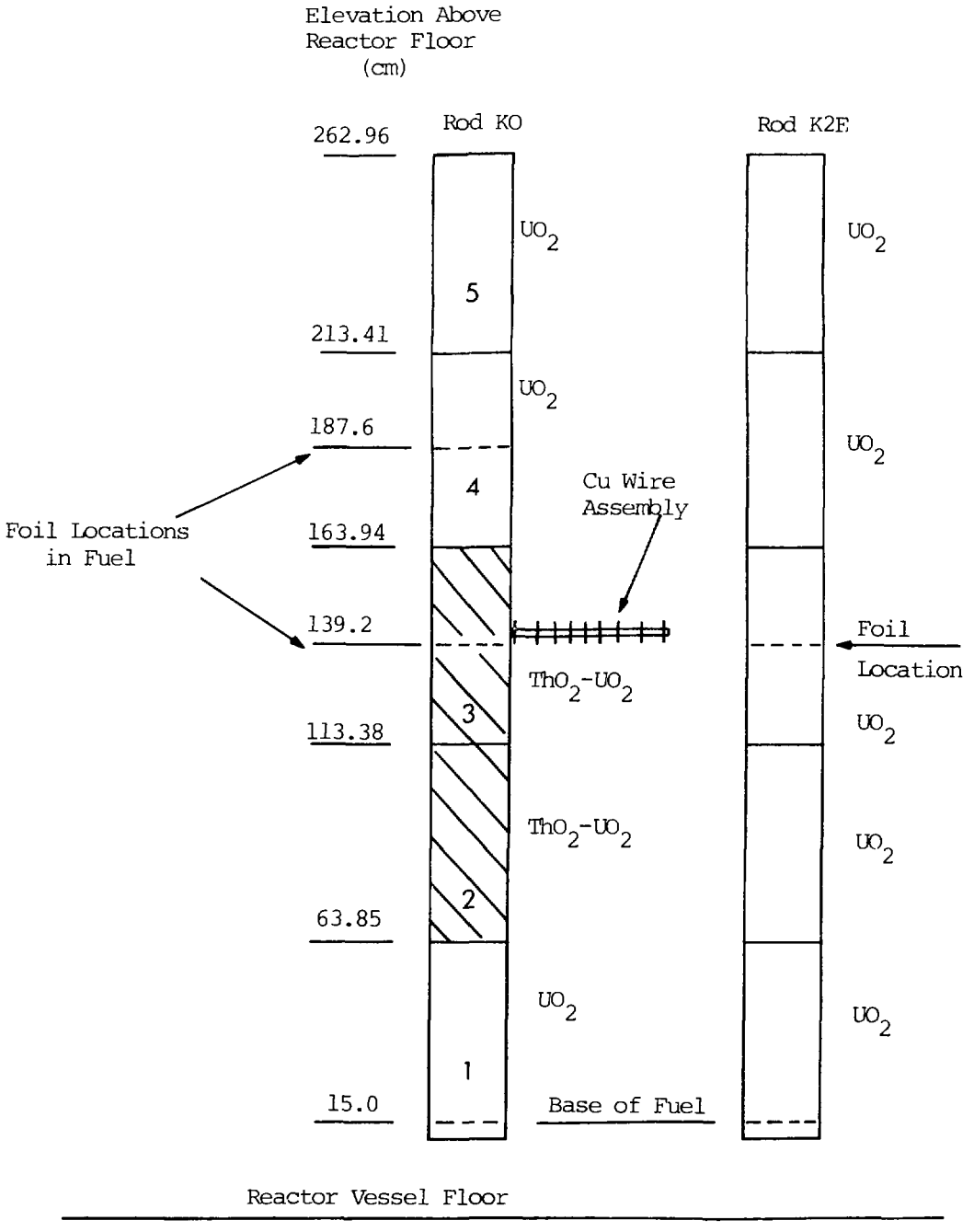

Figure 9: Detector Axial Measurement Locations in the Central Cell

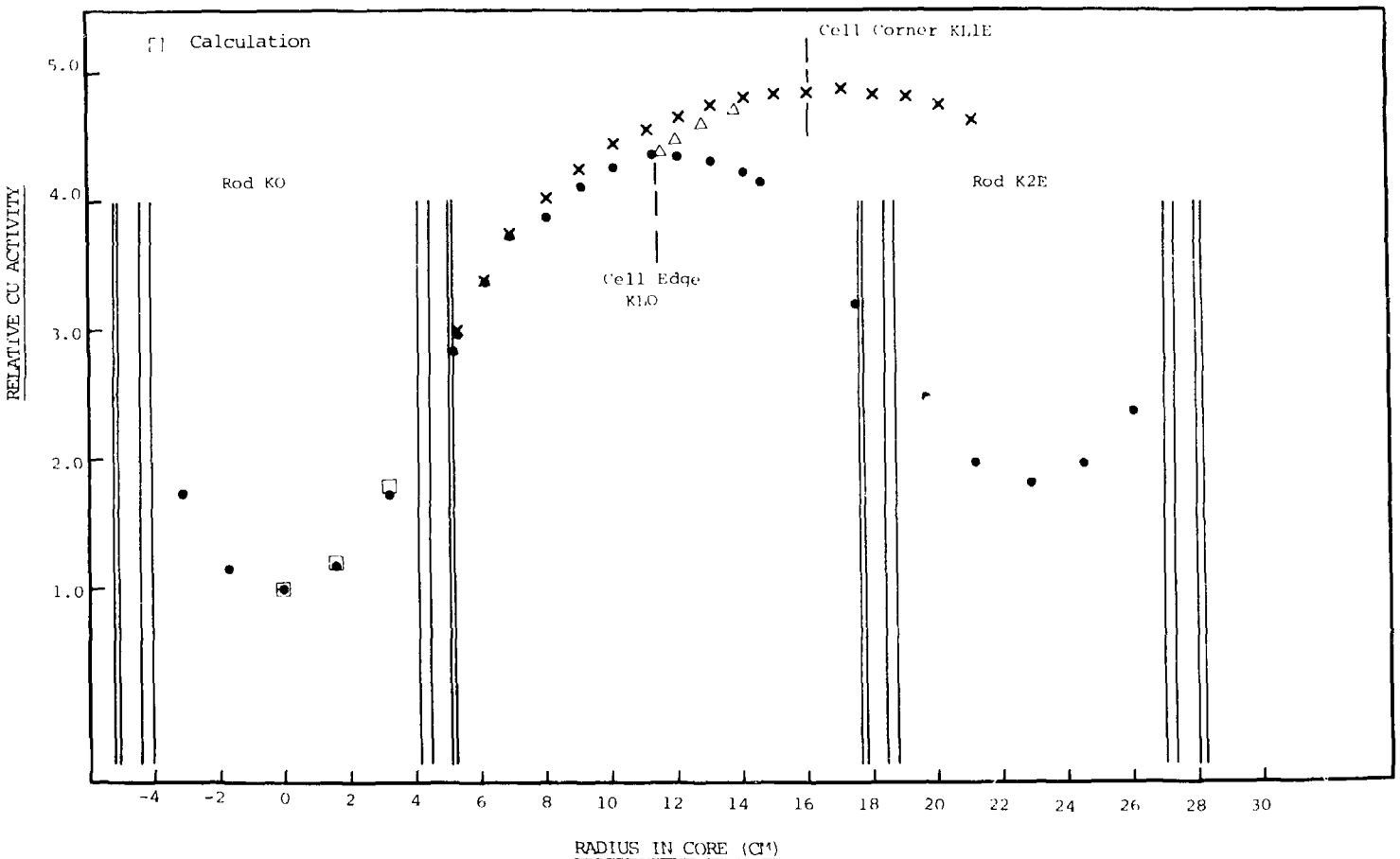

Figure 10: Central Cell Copper Activity Distribution: Two TnO_2-UO_2 Replacing UO_2 at Core Center.

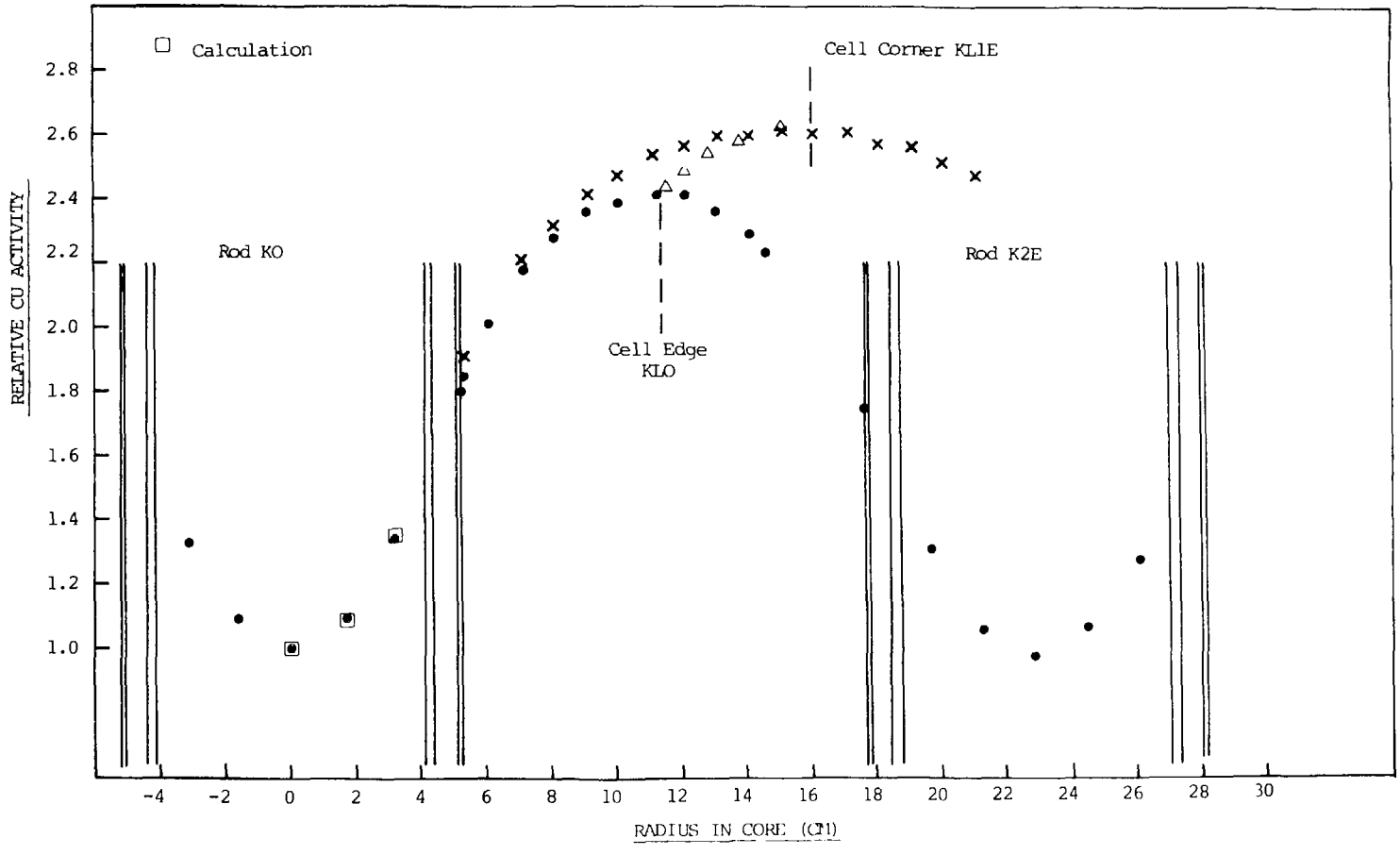

Figure 11: Central Cell Copper Activity Distribution: Natural UO_2 at Core Center.

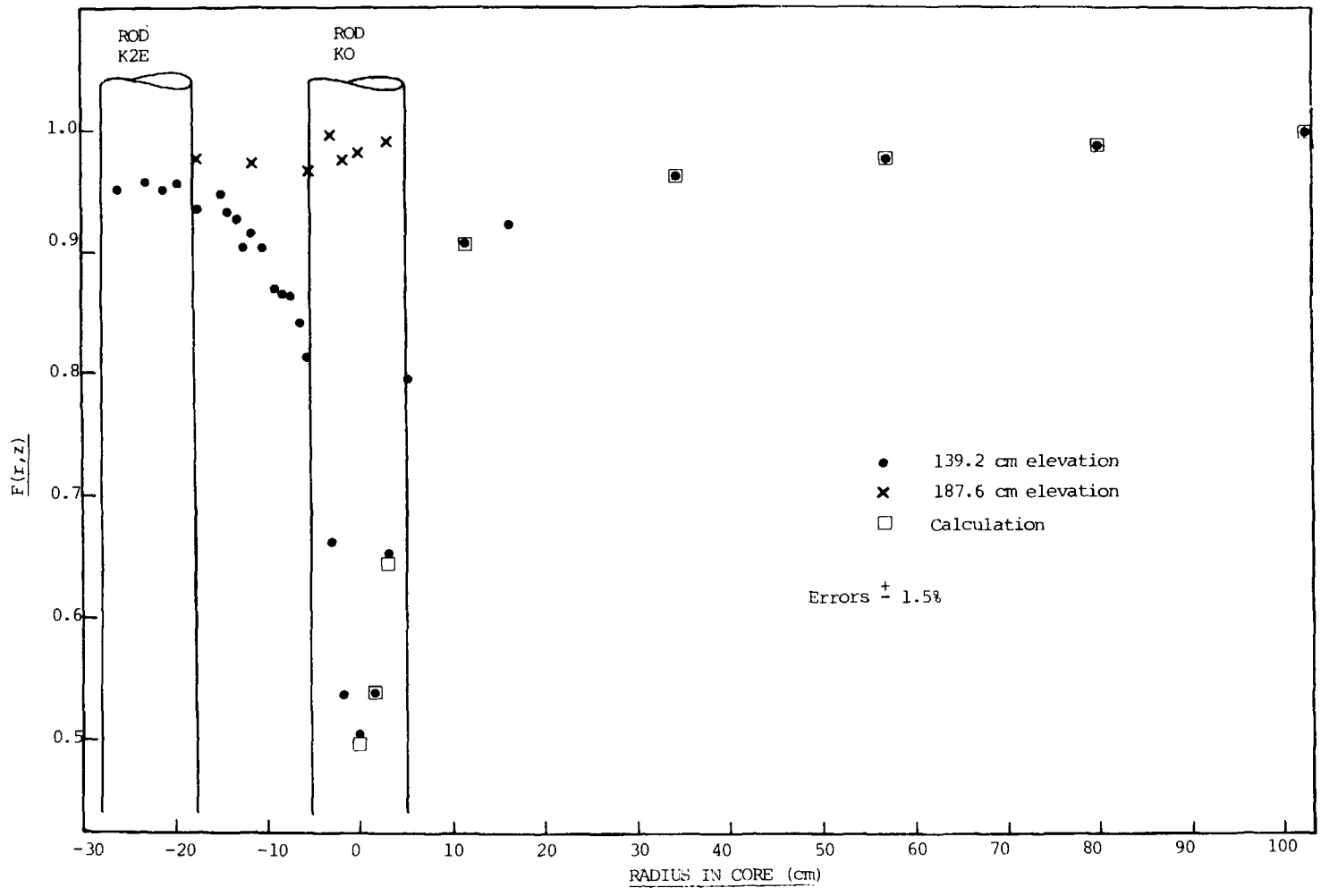

Figure 12: Radial Flux Perturbation Factor Results

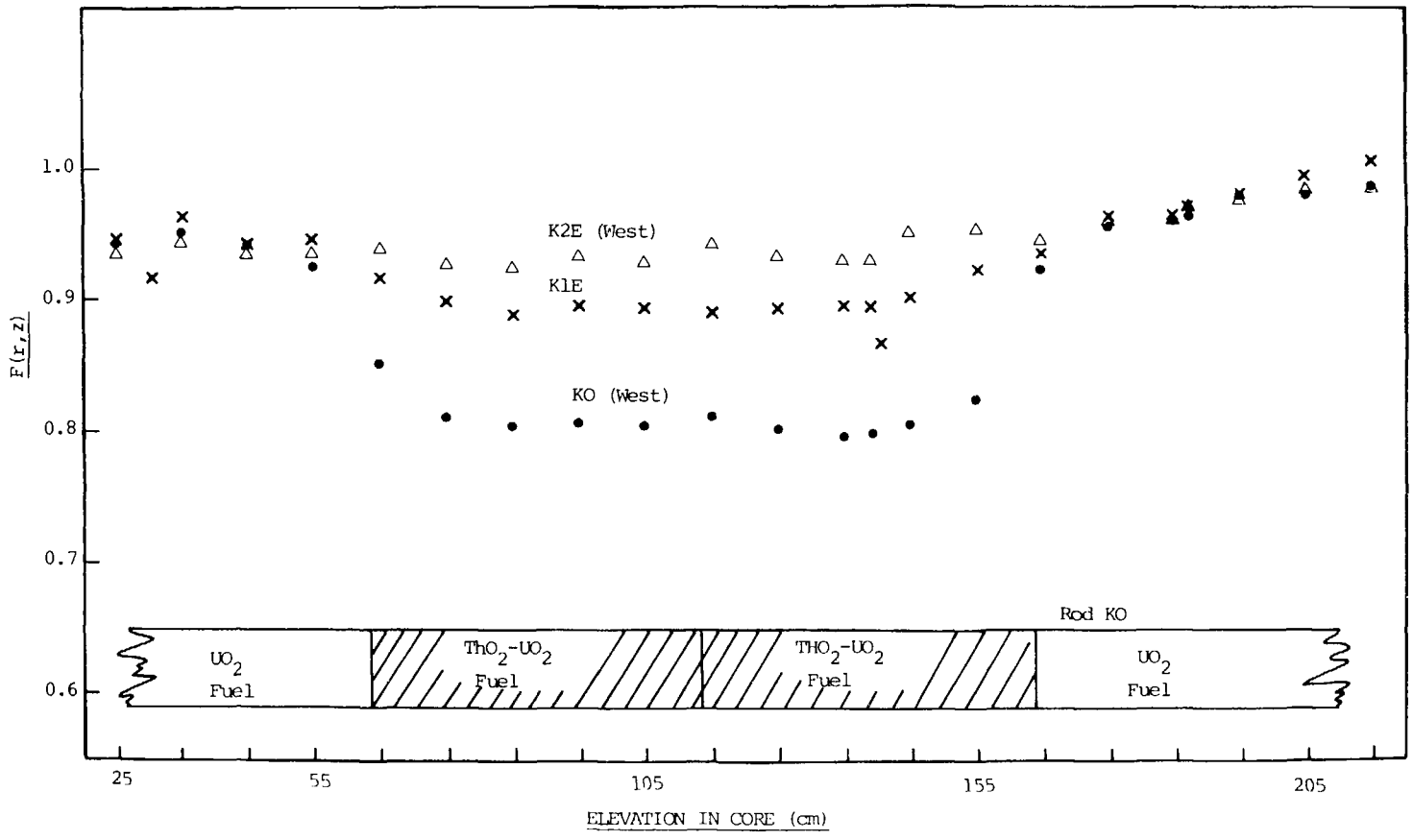

Figure 13: Axial Flux Perturbation Factor Results.

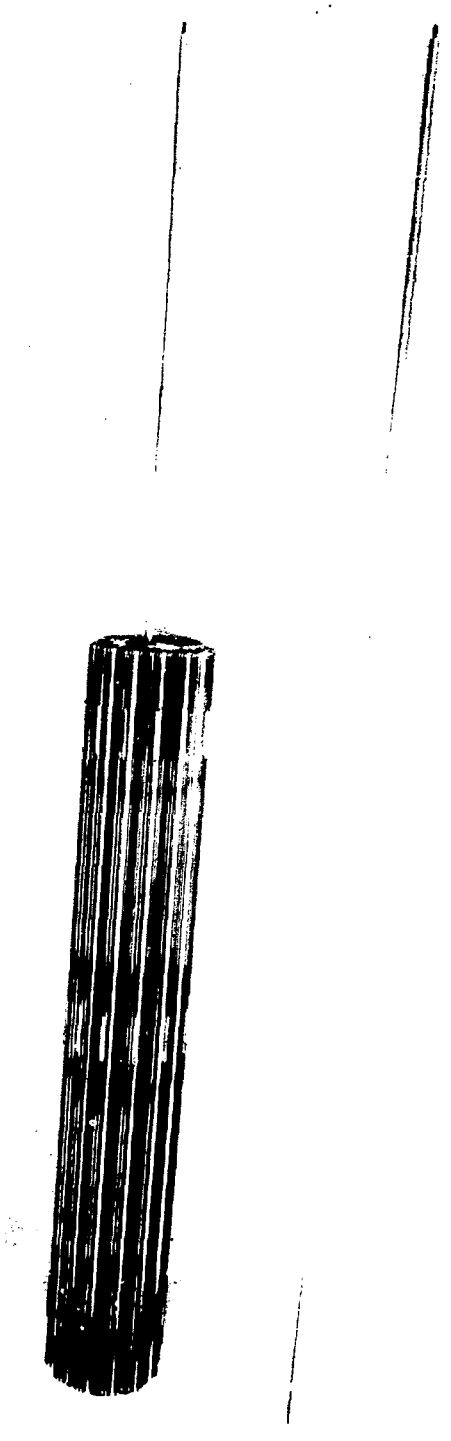

Figure 14: Flux Peaking Factor Measurement Wire Assembly

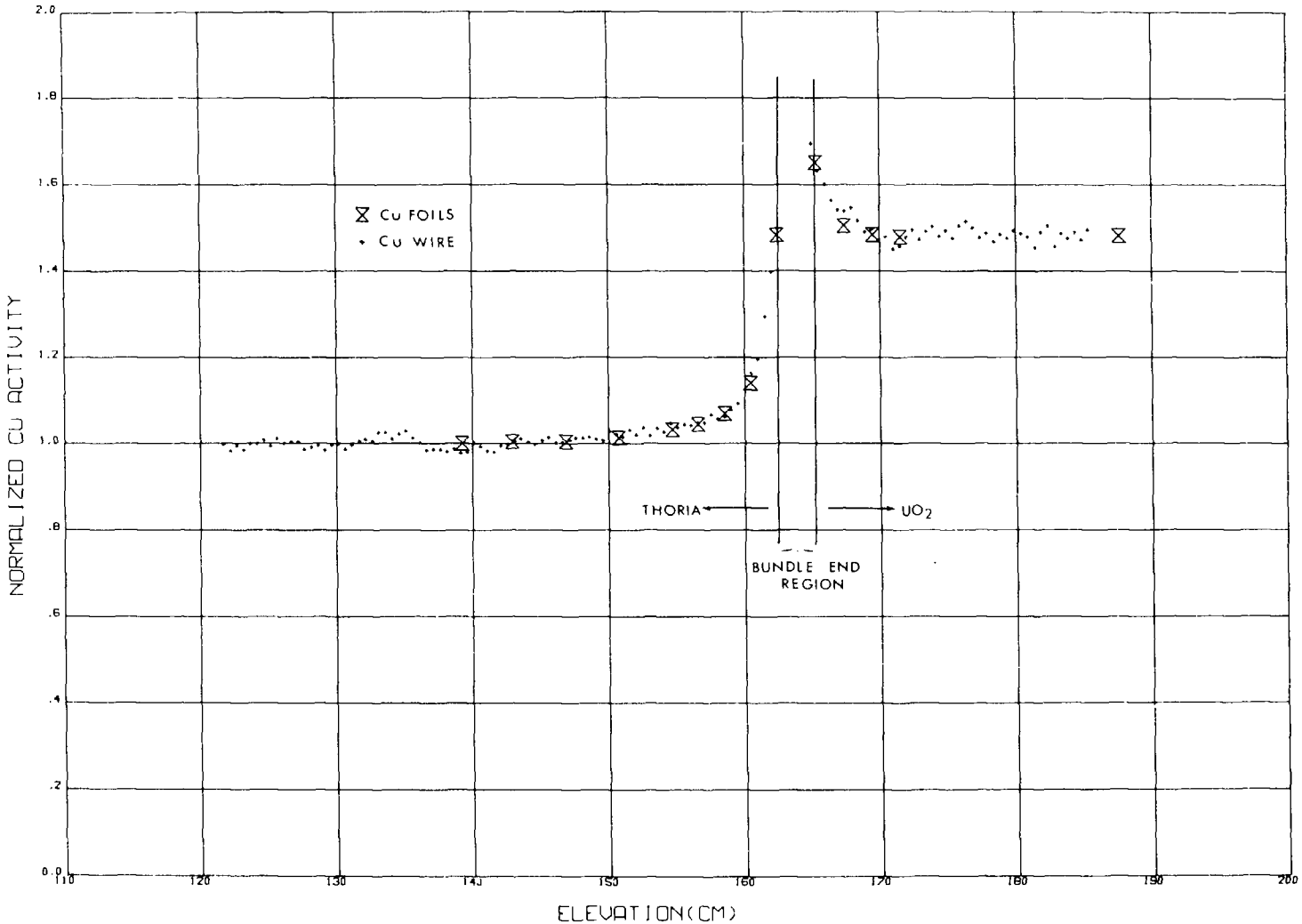

Figure 15: Demountable Bundle Outer Element Axial Activity Distribution Inferred from Normalized Copper Wire Activities.

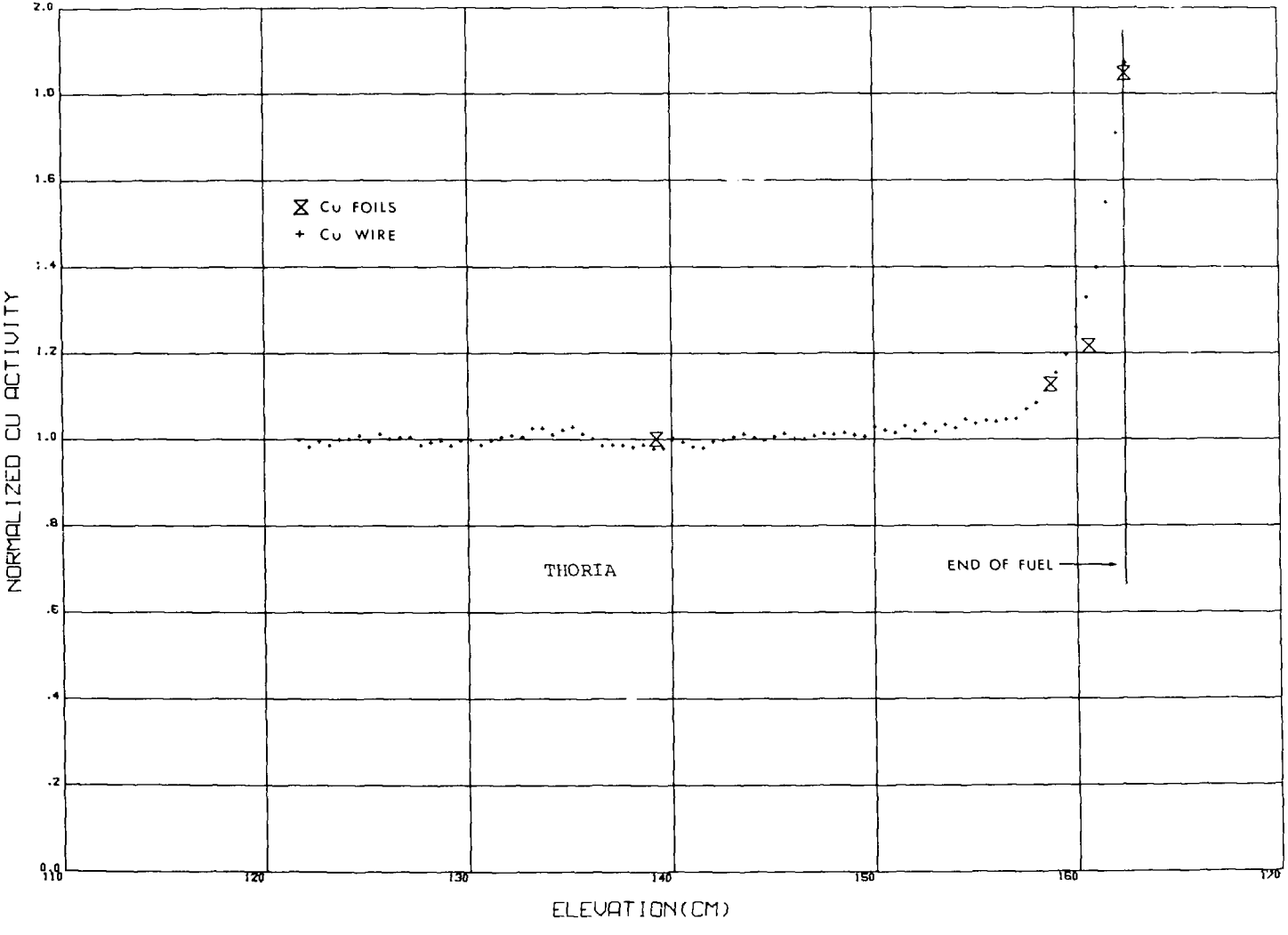

Figure 16: Demountable Bundle Intermediate Element Axial Activity Distribution Inferred from Normalized Copper Wire Activities.

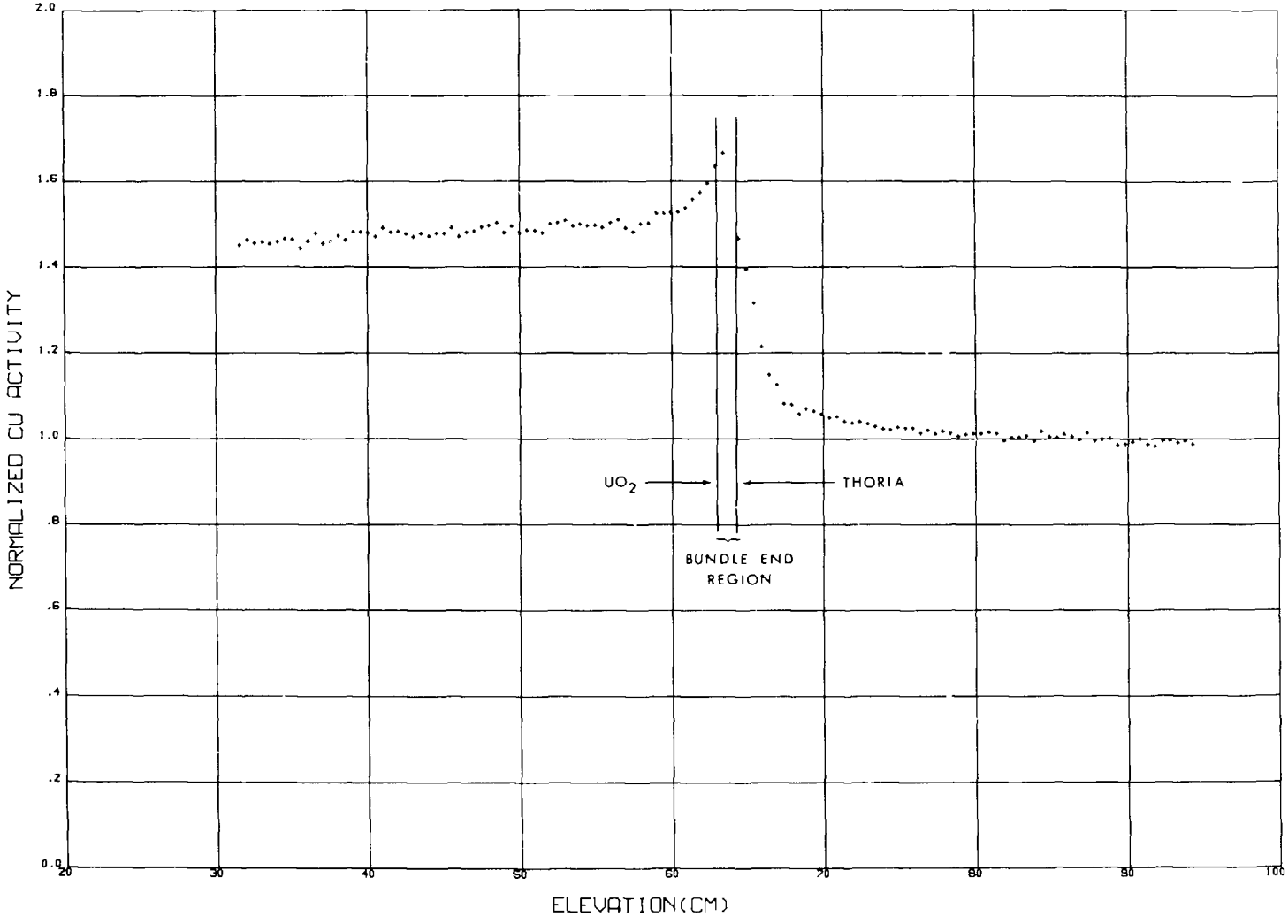

Figure 17: Production Bundle Outer Element Axial Activity Distribution Inferred from Normalized Copper Wire Activities.

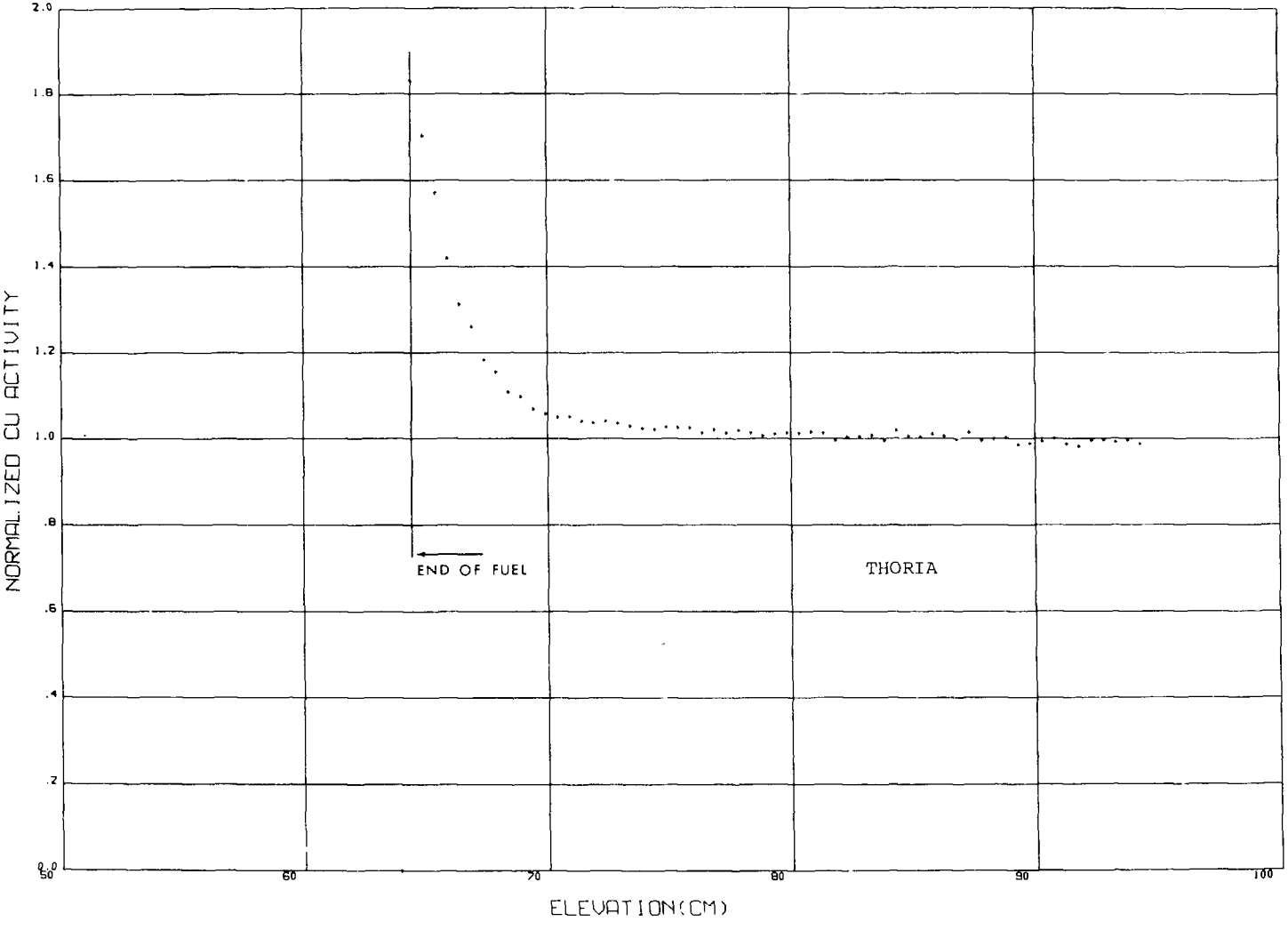

Figure 18: Production Bundle Intermediate Element Axial Activity Distribution Inferred from Normalized Copper Wire Activities.

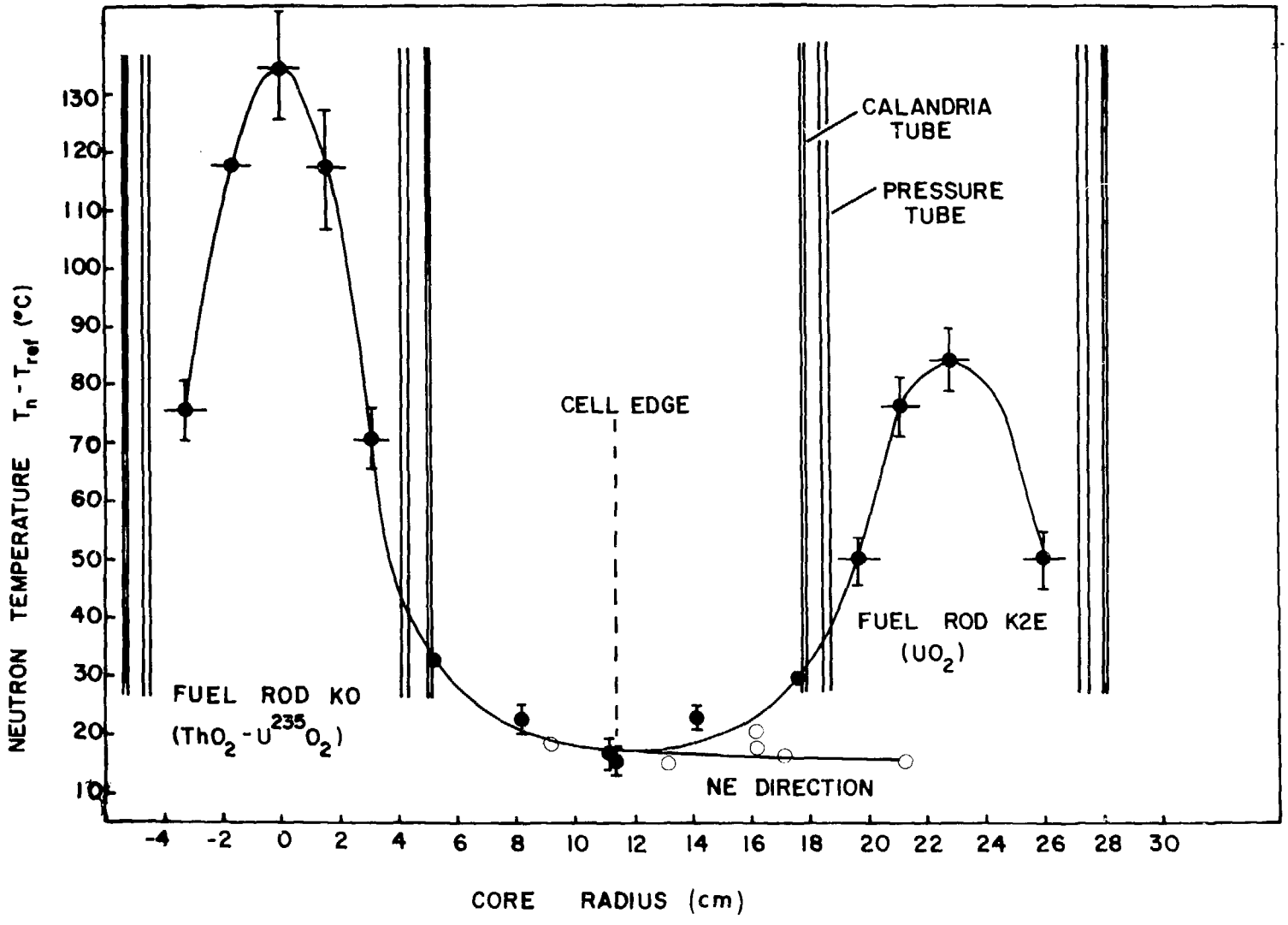

Figure 19: Neutron Temperature Distribution in Central Cell.

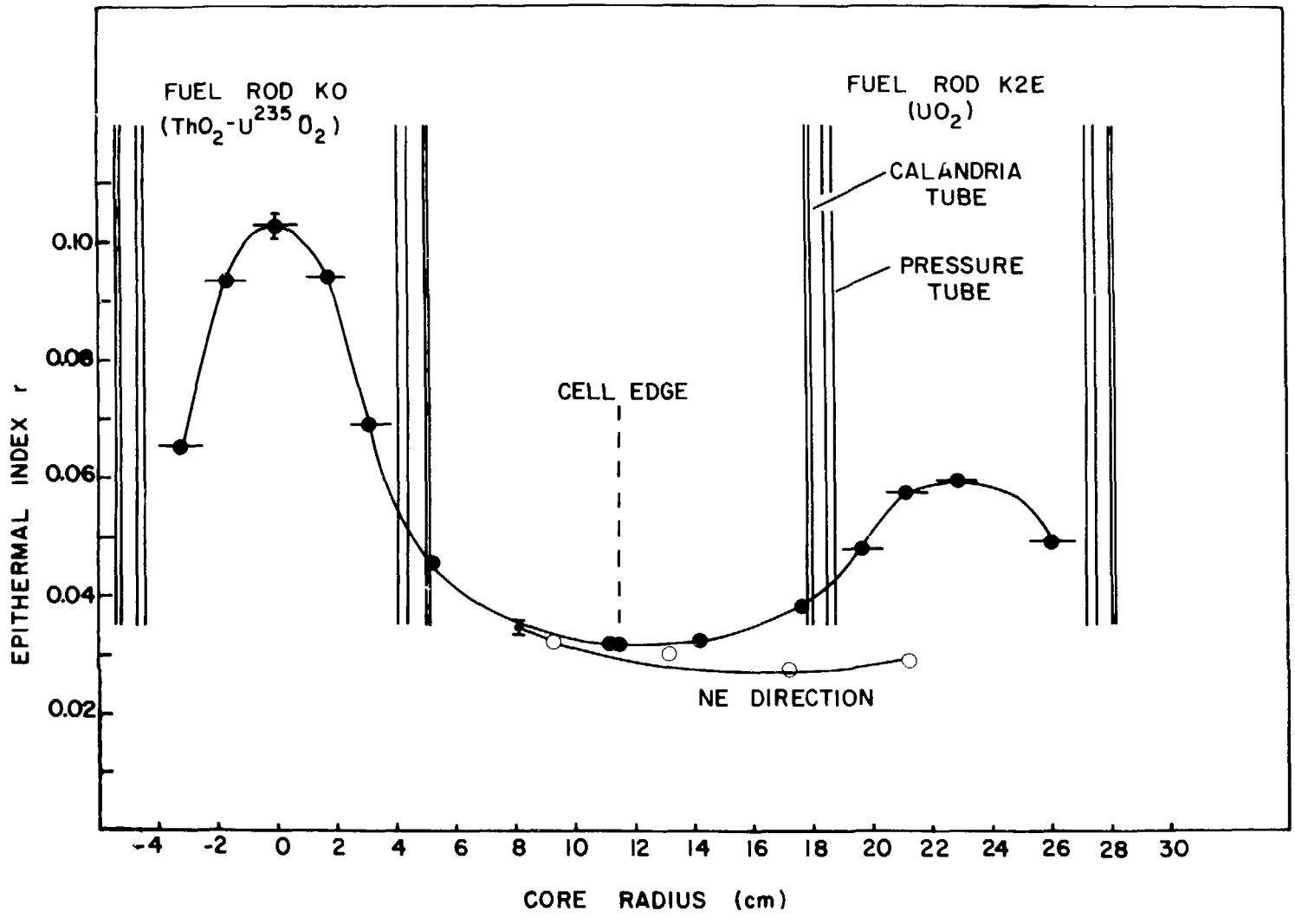

Figure 20: Epithermal Index Distribution in Central Cell.

ISSN 0067 - 0367

To identify individual documents in the series we have assigned an AECL- number to each.

Please refer to the AECL- number when requesting additional copies of this document

from

Scientific Document Distribution Office
Atomic Energy of Canada Limited
Chalk River, Ontario, Canada
K0J 1J0

Price $4.00 per copy

ISSN 0067 - 0367

Pour identifier les rapports individuels faisant partie de cette série nous avons assigné un numéro AECL- à chacun.

Veuillez faire mention du numéro AECL- si vous demandez d'autres exemplaires de ce rapport

au

Service de Distribution des Documents Office
L'Energie Atomique du Canada Limitée
Chalk River, Ontario, Canada
K0J 1J0

Prix $4.00 par exemplaire

0763-85